water

MDPI

Article

Submarine Geomorphology of the Southwestern Sardinian Continental Shelf (Mediterranean Sea): Insights into the Last Glacial Maximum Sea-Level Changes and Related Environments

Giacomo Deiana [1,3], Luciano Lecca [1], Rita Teresa Melis [1], Mauro Soldati [2], Valentino Demurtas [1,*] and Paolo Emanuele Orrù [1,3]

[1] Department of Chemical and Geological Sciences, University of Cagliari, 09042 Monserrato, Italy; giacomo.deiana@unica.it (G.D.); leccal@unica.it (L.L.); rtmelis@unica.it (R.T.M.); orrup@unica.it (P.E.O.)
[2] Department of Chemical and Geological Sciences, University of Modena and Reggio Emilia, 41125 Modena, Italy; mauro.soldati@unimore.it
[3] CoNISMa Interuniversity Consortium on Marine Sciences, 00126 Roma, Italy
* Correspondence: valentino.demurtas@unica.it

Abstract: During the lowstand sea-level phase of the Last Glacial Maximum (LGM), a large part of the current Mediterranean continental shelf emerged. Erosional and depositional processes shaped the coastal strips, while inland areas were affected by aeolian and fluvial processes. Evidence of both the lowstand phase and the subsequent phases of eustatic sea level rise can be observed on the continental shelf of Sardinia (Italy), including submerged palaeo-shorelines and landforms, and indicators of relict coastal palaeo-environments. This paper shows the results of a high-resolution survey on the continental shelf off San Pietro Island (southwestern Sardinia). Multisensor and multiscale data—obtained by means of seismic sparker, sub-bottom profiler chirp, multibeam, side scan sonar, diving, and uncrewed aerial vehicles—made it possible to reconstruct the morphological features shaped during the LGM at depths between 125 and 135 m. In particular, tectonic controlled palaeo-cliffs affected by landslides, the mouth of a deep palaeo-valley fossilized by marine sediments and a palaeo-lagoon containing a peri-littoral thanatocenosis (18,983 ± 268 cal BP) were detected. The Younger Dryas palaeo-shorelines were reconstructed, highlighted by a very well preserved beachrock. The coastal paleo-landscape with lagoon-barrier systems and retro-littoral dunes frequented by the Mesolithic populations was reconstructed.

Keywords: submarine geomorphology; morphostratigraphy; sea-level changes; Last Glacial Maximum; Sardinia; Italy

Citation: Deiana, G.; Lecca, L.; Melis, R.T.; Soldati, M.; Demurtas, V.; Orrù, P.E. Submarine Geomorphology of the Southwestern Sardinian Continental Shelf (Mediterranean Sea): Insights into the Last Glacial Maximum Sea-Level Changes and Related Environments. *Water* **2021**, *13*, 155. https://doi.org/10.3390/w13020155

Received: 27 November 2020
Accepted: 4 January 2021
Published: 11 January 2021

1. Introduction

Sea-level variations connected to climatic oscillations [1] cause changes in the landscape of coastal areas and continental shelves [2]. The comparative geomorphological analysis of emerged and submerged areas is particularly effective for revealing the land- and seascape changes [3,4]. Landscape evolutionary phases can be reconstructed considering morphostructural and morphostratigraphic settings and using geomorphological, seismic, sedimentological, palaeontological, and isotopic data. The detailed reconstruction of the submerged coastal palaeo-landscape is useful to understanding the dynamics of the human population during the Last Glacial Maximum (LGM) [5,6]. As such, marine and continental geomorphological analyses are crucial for better representing and understanding the Pleistocene landscape evolution [3,7–11].

This study aims to obtain new insights into the palaeo-geographic evolution of the San Pietro continental shelf of southwestern Sardinia (Figure 1) during the last cold stage

(MIS 2) by analysing erosional and depositional landforms formed during the LGM sea-level lowstand, as well as the palaeo-geographic coastal evolution connected to the LGM sea-levels. Several studies used different methodological approaches and analysed various palaeo-sea-level indicators (e.g., palaeo-cliffs, lowstand depositional terraces, beachrocks, fossiliferous deposits) to evaluate the post-glacial sea levels in the Mediterranean Sea in the past 20 ka. Previous studies also successfully applied the glacial-hydro-isostatic adjustment (GIA) models [12–17].

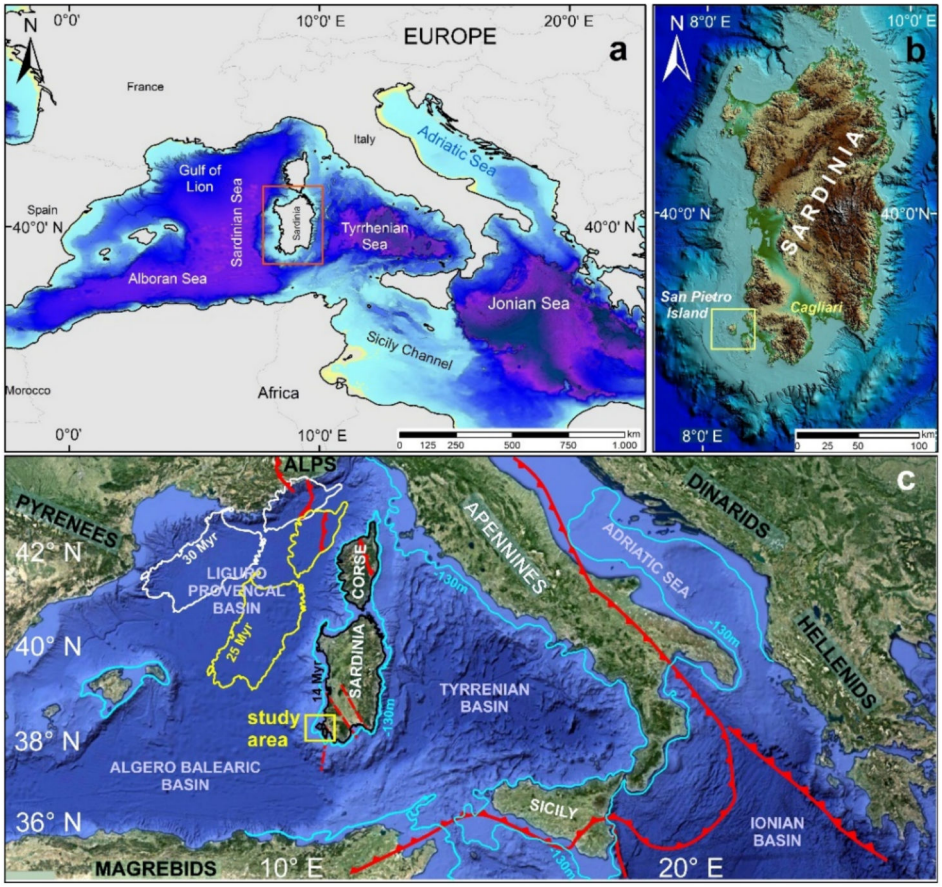

Figure 1. Geographic location and structural setting of the study area: (**a**) Sardinia Island within the Mediterranean Sea; (**b**) San Pietro Island on the SW side of Sardinia; (**c**) structural sketch map of the Mediterranean area. Red lines mark thrust fronts; white line the Sardinian-Corse block translation 30 Myr BP; yellow line Sardinian-Corse block translation 25 Myr BP (mod. after Carminati and Doglioni, 2008 [18]); Black line the Sardinian-Corse block translation 14 Myr (Gattacceca et al., 2007 [19]); Light blue color line, isobath of −130 m represents the coastline during the Last Glacial Maximum (LGM).

LGM shorelines are known from other areas of the Mediterranean Sea, including the Adriatic continental shelf [17,20–22], southern Tyrrhenian margin offshore Sicily [22–26], Calabria [27], and Malta [2,11,28,29].

For example, morphobathymetric data acquisition (i.e., high-resolution multi-beam and seismic data) integrated with direct survey methods (i.e., remotely operated vehicle (ROV) and diving) allowed scientists to obtain a particularly rich database of the south-western Sardinian continental shelf [30–35].

Herein, we analysed the structural and volcanic geological settings linked to the Oligo-Miocene rifting of the western Mediterranean and Sardinian-Corsican blocks to highlight the geomorphological features of the continental shelf surrounding San Pietro Island. These data contribute to the knowledge of the coastal palaeo-landscape and its evolution from LGM to the Holocene (Figure 1a,b). In particular, submerged high rocky

coast morphotypes, a large palaeo-valley, a palaeo-lagoon and the successive phases of post-glacial sea level stationing were analyzed.

2. Geological and Structural Settings

The southwestern continental margin of Sardinia is characterised by normal faults that define intrashelf and intraslope basins [36]. This part of the Sardinian continental margin has been explored using geophysical surveys and deep drills, defining the order and geometry of the depositional sequences [36–41] (Figure 1c). High-angle normal fault systems characterised the western Sardinia continental margin setting between the Middle-Upper Oligocene and Miocene when, owing to the Apennine-Maghrebian chain orogeny, the intra-back arc basins opening caused the formation of an extensive system of rifts [42–45]. The genesis of the margin was clarified based on the ECORS-CROP Programme seismic data by examining the extensional tectonic inversion of a compressive structure of the Pyrenean western branch (Figure 1c) [39].

The margin formed as the transition between the western Mediterranean rift and the western branch of the Sardinian rift system and later assumed the structural and evolutionary characteristics of a divergent margin [36] (Figure 2). The kinematic analysis of the central Mediterranean shows that the Sardinia-Corsica block rotated until about 15 Ma later it became almost stable [18,19]. However, in the western part of the base of the margin, a significant earthquake (38.21°–08.21°; 5.4 Mw) was recorded on in August 1977 [46]. Furthermore, the INGV (Istituto Nazionale di Geofisica e Vulcanologia) earthquake catalogue, which contains the seismic records for the past 25 years, shows three other major earthquakes in southern Sardinia: one earthquake with a magnitude of 5.5 in August 1988 along the Sant'Antioco active fault, from Toro Island to Quirino Seamount, and two earthquakes with a magnitude of 4.5 in March 2006 at the sea prolongation of a major fault NW–SE Campidano graben that marks the western edge of this Plio-Quaternary graben. Therefore, slight fault movements that produce an occasional seismicity are still present and affect the margin.

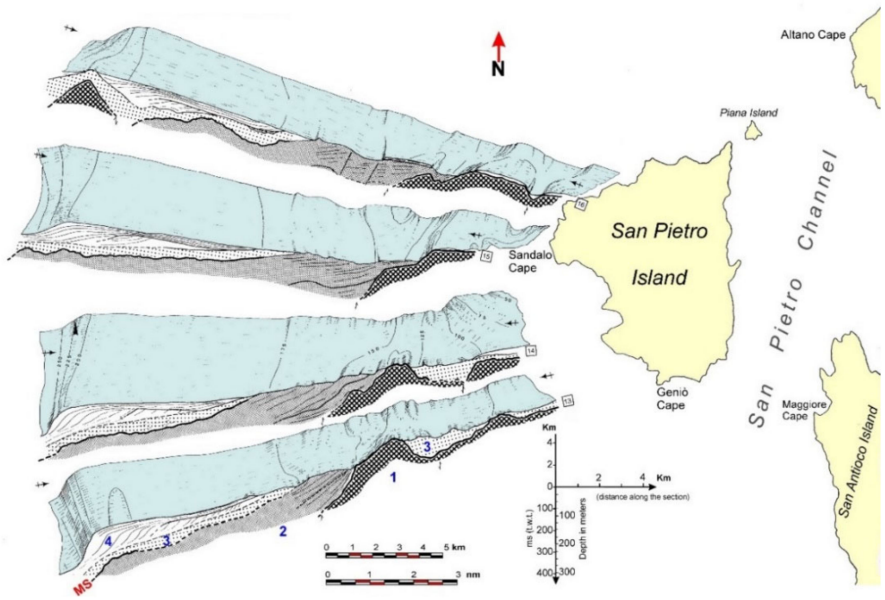

Figure 2. Sectioned block diagram of the Sardinian southwestern continental shelf off the San Pietro Island. (**1**) Acoustic basement (volcanic complex—Lower-Middle Miocene); (**2**) lower sedimentary sequence (Middle-Upper Miocene); MS) Messinian erosional surface; (**3**) sedimentary sequence poorly or not stratified in the lower part, with undulating stratification in the upper part (Lower-Middle Pliocene); (**4**) upper sedimentary sequence, prograding complex of the external platform, superficial deposits in the proximal platform (Upper Pliocene—Quaternary) (after Lecca, 2000 modified [36]).

The sedimentary units preceding the Oligo-Miocene Sardinian rifting stage are represented by the Palaeozoic basement, marine clastic Eocene series, and fluvial sandstones and claystones of the Cixerri Formation (Upper Eocene to Lower Oligocene). The initiation of the Oligo-Miocene rifting was accompanied by the andesitic volcanism (Upper Oligocene to Aquitanian) of the Sulcis block. The subsiding basin was filled by the fluvial sediments of the Ussana Formation and the marine marly-arenaceous and carbonate sediments of the Lower Miocene [42].

The continental margin off San Pietro Island is characterised by a steep slope, which extends to the Sardinian-Balearic abyssal plain to a depth of approximately 2800 m [41]. The inner and intermediate continental shelf is characterised by the extensive outcrops of volcanic rocks, consisting of ignimbrites (comendites) and pyroclasts [35]. From a geochemical point of view, the rhyolites predominate, while the dacites characterise the basal volcanic formations [43,47]. Explosive volcanic eruptions occurred on San Pietro Island during the Burdigalian, Miocene (15–17 Ma). From a morphostructural point of view, the ignimbrite outcrops are characterised by wide mega-cuestas, calderas, necks, and dikes (Figure 2) [35].

The presence of the Oligo-Miocene volcanites at the tectonic block boundaries is marked by magnetic anomalies on the inner continental shelf [43] and was documented by analysing the rock samples from the lower margin of the Seamount Quirino [36] (Figure 3). On the distal shelf, the Miocene volcano-sedimentary and sedimentary strata rest on the volcanic substrate. The Miocene sedimentary sequence, up to the pre-evaporitic Tortonian marls, tends to be characterised by an erosional surface tied up to the Messinian eustatic fall [48]. In the lower part of the Miocene sedimentary sequence, the clinoform reflections are spaced wider, and the ages close to the Burdigalian are suggested [36] (Figure 4).

3. Geomorphological Setting

The major factor controlling the evolution of submarine canyons in the Mediterranean basin is the Messinian salinity crisis, which induced a significant forced sea-level fall of approximately 2000 m from the present-day sea level [42]. The consequent emergence of the continental margin led to intense erosion [37,48,49]. The following Pliocene flooding event deposited a thick mud drape over the entire continental shelf [7].

The shelf break is located at depths of 190–220 m and hosts the Plio-Quaternary prograding sedimentary wedge [35]. Both the shelf break and the Upper continental slope are eroded by the canyon heads formed via the retrogressive erosion processes. Intrachannel landslides are observed in the canyon sidewalls, while the Upper continental slope is distinguished by creeping areas and complex landslides often associated with pockmark fields due to fluid emissions [34,50].

The Messinian eustatic sea-level fall has been recognised on the Sparker seismic tracks acquired during the MAGIC (Marine Geohazard Along Italian Coasts) Sardinia Channel 2009 survey off Cala Fico. That study identified a palaeo-valley with polycyclic evolution that engraved both the volcanic substrate and the lower sedimentary sequence. Convoluted and plane parallel reflectors seem to characterise the Quaternary sequence.

Arenaceous beachrocks are represented by two extensive outcrops located to the north of La Punta and Piana Island at depths of 45–50 m. The outcrops display prominent erosion features both on the top surface and at their edges [51] (Figures 3 and 4).

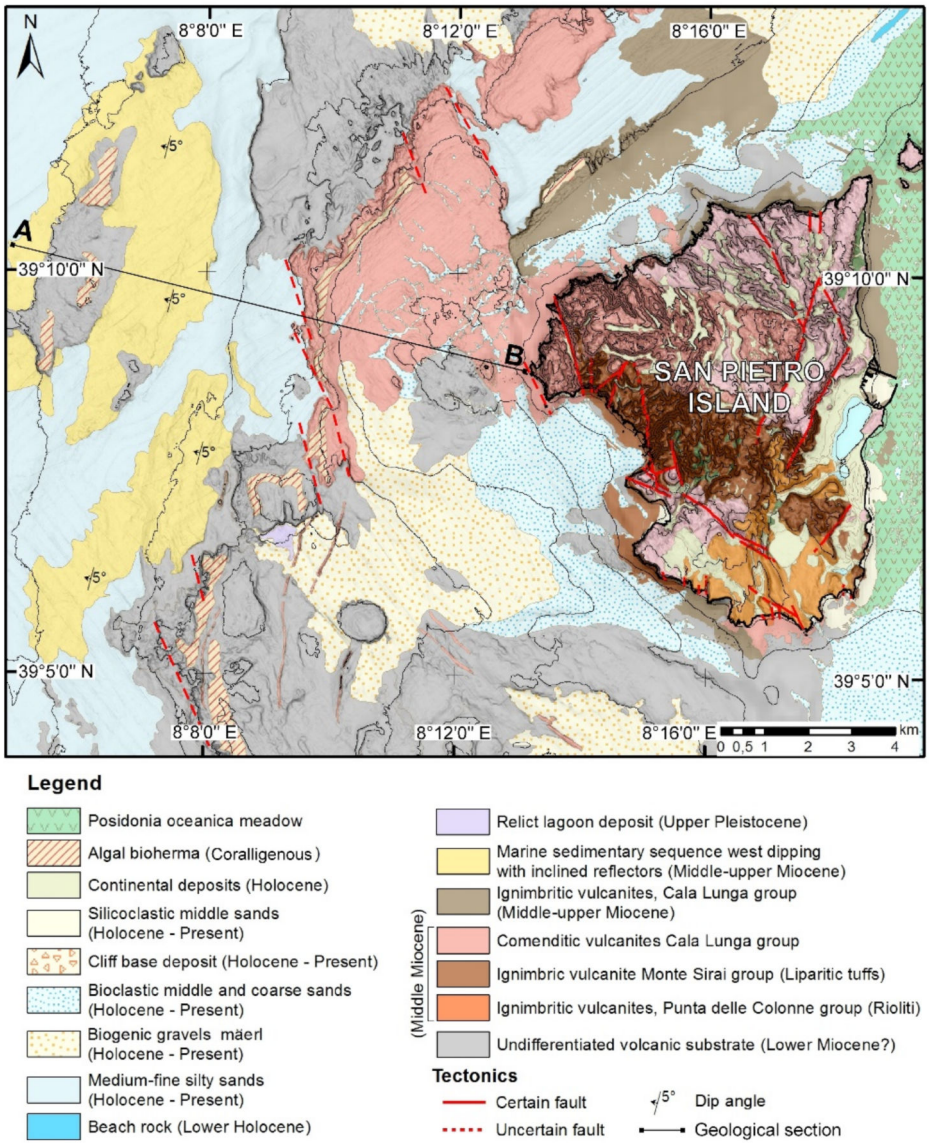

Figure 3. Geolithological sketch map of study area from the Geological Map of Italy. Scale 1:50,000—Sheet 563 "Isola di San Pietro" (Rizzo et al., 2015 [35]).

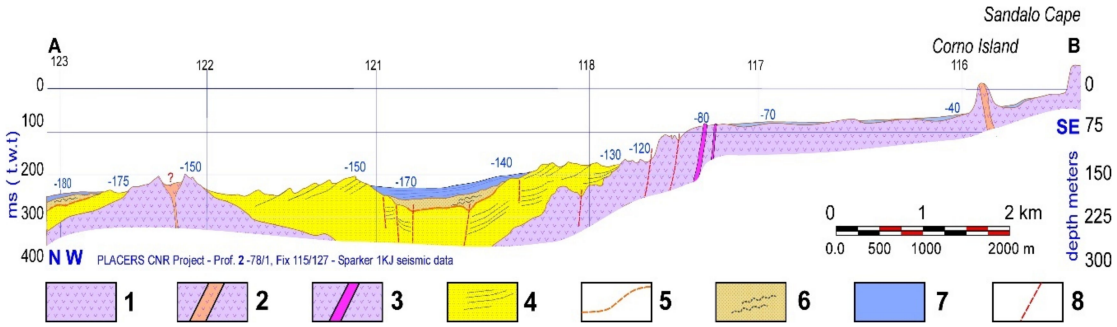

Figure 4. Geological section from seismic data of: Oceanography and Seabed—Mineral Resources—PLACERS Project CNR—Profilo 2-78/1, Fix 115/127—Sparker 1KJ: (1) Volcanites (Lower-Middle Miocene; (2) emission chimney; (3) dikes; (4) marine sedimentary sequence with inclined reflectors (Middle-Upper Miocene; (5) Messinian erosional surface; (6) marine sedimentary sequence with undulated reflectors. (Pliocene-Pleistocene); (7) Holocene-current drape; (8) fault.

The beachrocks are slightly tilted seaward, presenting a typical character of beach sand bodies, with the sedimentary structures (e.g., parallel lamination and wedge-shaped, sigmoidal, and inclined stratification) common for coastal environments [52].

Considering the outcrop depth, these beachrocks are attributed to the end of the Younger Dryas event and are interpreted to be formed when the eustatic sea level dropped during the Pleistocene–Holocene marine transgression.

The actual and subactual sediments on the distal continental shelf off San Pietro Island are represented by pelitic sands and sandy pelites. These deposits contain variable bioclastic fractions, composed of foraminifera and the degradation products of algal bioherms. These algal bioherms colonise the rocky substrate and can be found both outcropping and suboutcropping [35] (Figure 2).

The Middle continental shelf has medium-grained, slightly pelitic sands, which bioclastic component increases towards the lower limit of *Posidonia oceanica* meadows. The areas farther offshore are dominated by biogenic gravels consisting of red algae (mäerl). These gravels form patches and hydraulic dunes. The near-continental shelf and the peri-littoral area are dominated by deposits linked to the retreat of high rocky coasts. In particular, base cliff deposits consist of sub-rounded heterometric blocks of volcanic lithology and landslide deposits with isolated sub-angular mega-blocks. The submerged beaches are characterised by medium- to coarse-grained sands with a predominantly quartz composition, whereas medium- and fine-grained sands are present in the bays of the southeastern sector. The sandy deposits with a predominantly quartz composition are located near the shoreline and Upper limit of the *Posidonia oceanica* prairie and have an important carbonate bioclastic fraction.

The first studies published on the LGM palaeo-shoreline of the western Sardinian shelf were conducted northward of our study area and indicated the existence of both erosional landforms and sedimentary sequences, in distal continental shelf, at depths between −120 and −140 m [53–56].

4. Materials and Methods

4.1. Seismic Data

The dataset used herein includes the seismic analogic data (Sparker 0.8 KJ) and by a high-resolution 3.5 kHz seismic sub-bottom profiler. These data were purchased from R/V Bannock (CNR) and collected during the oceanographic cruise "Placers 78/1" as part of the "Oceanografia e Fondi Marini" project. These data allowed the reconstruction of the Upper continental margin geological structure [36].

In order to reconstruct the palaeo-geomorphological setting, in particular, the intermediate continental shelf palaeo-hydrography, digital seismic surveys were carried out by R/V "Universitatis" during the oceanographic cruise "Canale di Sardegna 2009" in the frame of the MAGIC Project. The seismic surveys used a seismic energy source (Sparker 100/1000 J, Applied Acoustic CSP 20200, Great Yarmouth, United Kingdom), while the sub-bottom surveys aimed to reveal the structure of the surface deposits and were carried out using a geoacoustic source (Geochirp II-CP931, GeoAcoustics–Kongsberg, Great Yarmouth, United Kingdom) (Figure 5).

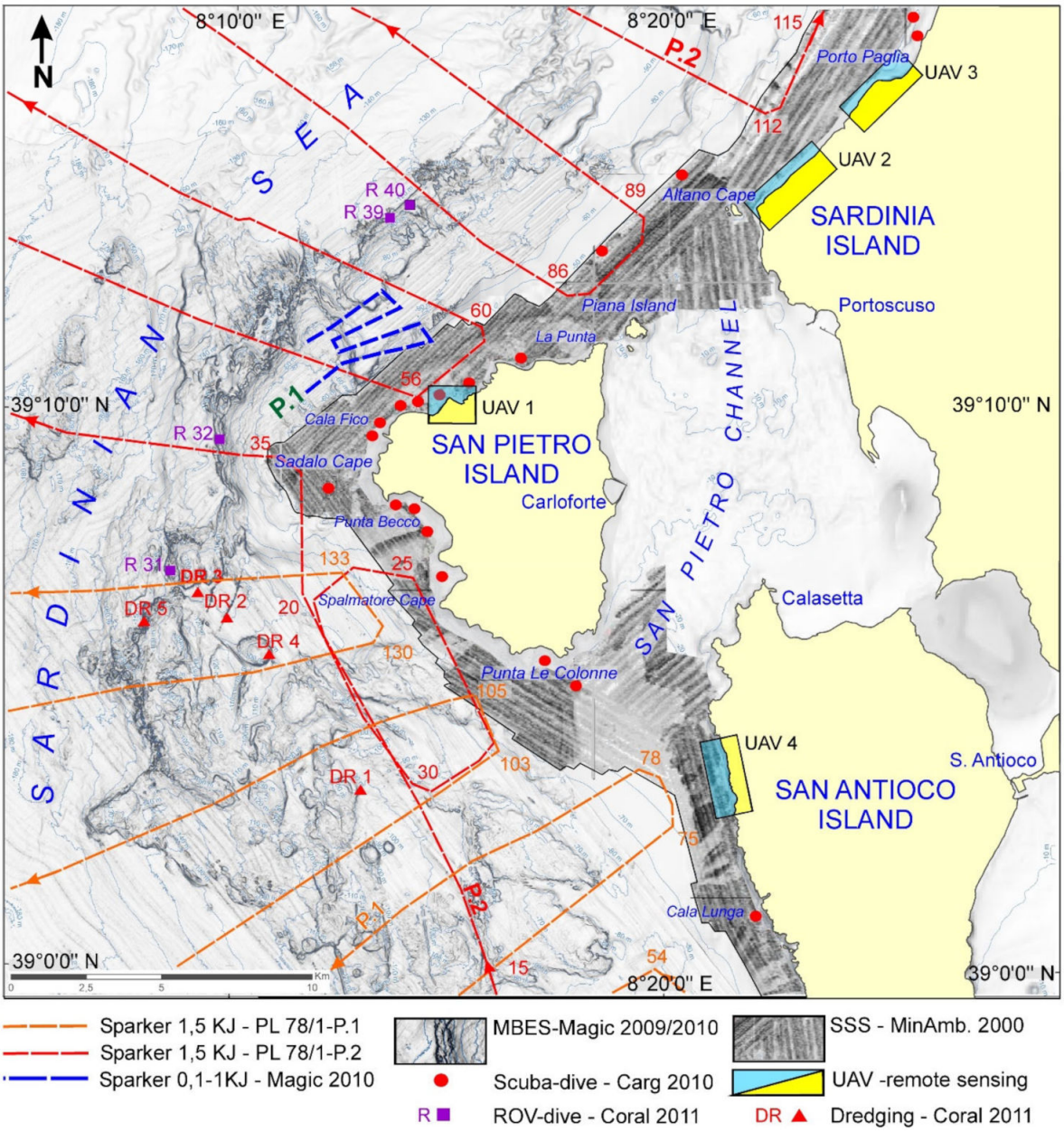

Figure 5. Data locations: spatial coverage multi-beam echosounder (MBES), side scan sonar (SSS) and uncrewed aerial vehicle (UAV); seismic profiles, scuba-dive and ROV stations; dredging sampling points.

4.2. Multibeam, Singlebeam, and Side-Scan Sonar Data

Morphobathymetric data were acquired during the oceanographic cruises "Canale di Sardegna 2009" and "Sardegna 2010" using R/V "Universitatis CoNISMa" as part of the Marine geohazard along Italian coasts (MAGIC) Project. The 50 kHz multi-beam echosounder (MBES, RESON SEABAT 8160) was calibrated with continuous sound velocity detection lines and vertical profiles. Onboard R/V Universitatis, the integrated system contained a motion sensor and gyro (IXSEA OCTANS) and a satellite differential GPS (Global Positioning System). The geocentric datum WGS84 and the UTM projection were chosen for navigation and display. The data collected during the survey were integrated with the Official National Italian Geological Cartography (CARG) project data.

Side-scan sonar data acquisition was performed on the proximal continental shelf with depths ranging from 10 to 50 m as part of the "Mapping of *Posidonia oceanica* meadows along the coasts of Sardinia" project funded by the Italian Ministry for the Environment on

R/V "Copernaut Franca". A 100–500 kHz, dual-frequency sensor was used with a towfish (Model 272/T, EG&G Marine Instruments, Massachusetts, USA) connected to the Triton Elics system (Triton Elics International, Portland, OR, USA) with ISIS software (Triton) for geo-referenced acquisition and Delf Map for the construction and correction of the mosaic. The correct positioning of the acquired data was ensured by a GPS receiver with differential correction (Trimble 5007, Sunnyvale, CA, USA).

In the coastal areas with depths of 5–20 m, single-beam echosounder and lateral sonar data were acquired using a towed sensor (1 MHz, Starfish 990, Tritech, Aberdeenshire, Scotland) and sonar (200/800 kHz, Lowrance Elite 12, Tulsa, Oklahoma) with a hull transducer (Lowrance Simrad Active, Tulsa, Oklahoma) (Figure 5).

4.3. Direct Seabed Observations

On the internal shelf, diving surveys and sampling were carried out during the surveys "San Pietro Sub 2006" and "San Pietro 2010" as part of the "Official National Italian Geological Cartography" project. Fifteen underwater survey stations were set down to a depth of 50 m. Direct observations aimed to elaborate the interpretative keys for the geophysical data. Two teams of four geologists were engaged in the underwater surveys. The first geomorphological survey data were reported on tablets equipped with a depth gauge.During the underwater survey, sediment sampling was carried out with a vacuum core, whereas rocks were sampled with a chisel and heavy hammer. Six cores of unconsolidated sediments, five sedimentary rock samples (beachrocks and eolianites), and 20 samples of acid volcanites were collected. The data were synthesised using special survey cards (Figure 6). Direct seabed observations in the distal shelf areas and, in particular, the exploration of the palaeo-cliff walls at depths of 85–140 m were conducted using ROV *Polluce* III R/V Astrea (ISPRA, Istituto Superiore Protezione e Ricerca Ambientale). These surveys were carried out as part of the "CORALLIUM RUBRUM" and "MARINESTRATEGY" projects, being sponsored by Italian Environmental Ministry—Autonomous Region of Sardinia. High-definition ROV images supported the habitat mapping of deep rocky bottoms dominated by red algal coralligenous assemblages and coral settlements (*Corallium rubrum* and *Leiopathes glaberrima*) [31,32]). These images allowed scientists to calibrate the geomorphological interpretation of palaeo-cliffs, especially regarding gravity-induced processes (Figure 5).

4.4. Dredging and Shell Sampling for Radiocarbon Analysis

The "SULCIS dredging survey" (2011) was conducted on the distal continental shelf, onboard R/V Gisella, using a classic submerged cylindrical dredger and two-cylinder experimental dredger. The dredging route was planned upon the analysis of morpho-bathymetric data and seismic profiles. The coordinates for the core sampling sites were determined using a differential GPS onboard the ship. The seabed depth at each core sampling point was acquired from the digital terrain models (DTM) processed using sonar multi-beam data. The volcanic rocks were not sampled because massive coralligenous bioconstructions with thicknesses greater than 50 cm covered them (Figure 5).

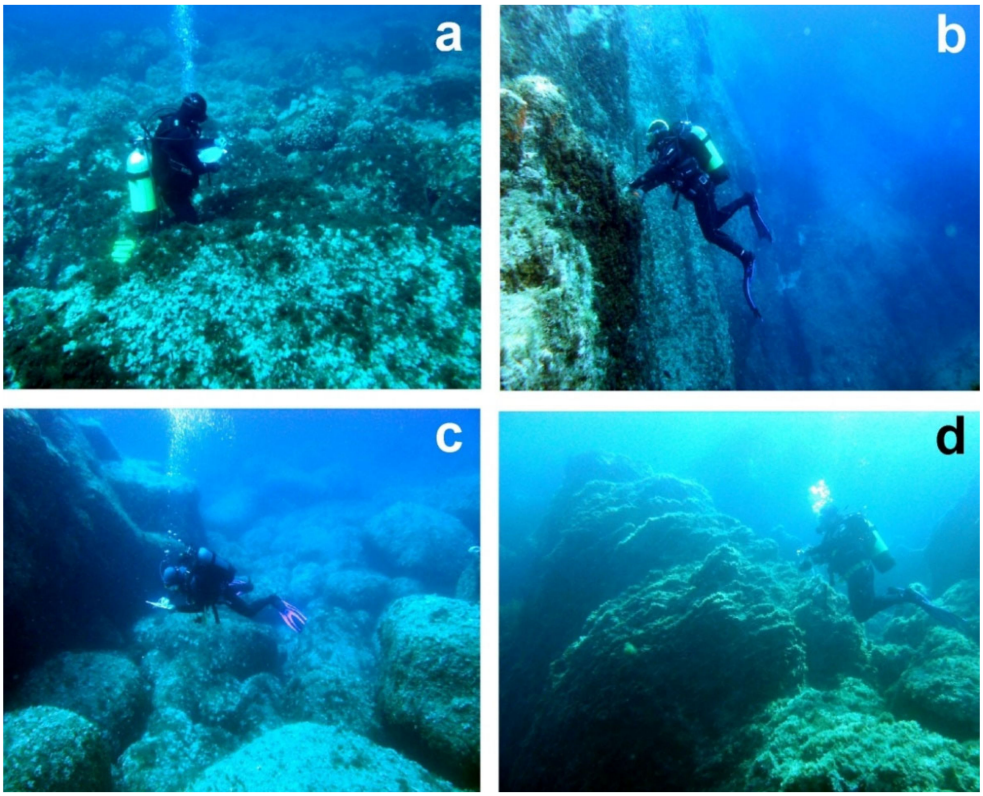

Figure 6. (**a**) Diver engaged in underwater geomorphological survey, using tablet with compass, clinometer, depth gauge and collimator at −15; (**b**) Fault mirror exhumed by erosion in Cala Fico at 10 m; (**c**) Foot cliff deposit with subspheroidal blocks at −18 m; (**d**) Lamination of pyroclastic lavas (Comenditi) in Cala Vinagra at 13 m.

4.5. Aerial and Uncrewed Aerial Vehicle Inland Remote Sensing

To obtain high-resolution aerial photos and topography suitable for the mapping of the onshore Sardinian coastal sector, we analysed the available topographic data produced by LiDAR (light detection and ranging) surveys. These aerial photogrammetric surveys were carried out by the Autonomous Region of Sardinia in 2008. The high-resolution aerial photos allowed us to analyse the coastal sector with high precision, down to a depth of 15 m. A cell size of 1 m and a mean vertical resolution DTM of approximately 30 cm were extracted.

In the most important sectors, such as the Capo Altano landslide, the surveys were performed with uncrewed aerial vehicles (UAVs, DJI Matrice 200, Shenzhen, Guangdong) equipped with a megapixel camera (ZENMUSE X5S 20.8). The survey was conducted by the UAVs flying at altitudes of 40–80 m above the ground level and maintaining a stable speed of 2.5 m/s. The acquired images were analysed and processed using the photogrammetric PhotoScan software (Agisoft, St. Petersburg, Russia). Being constrained by 12 ground control points, the resulting orthorectified mosaic and digital elevation model (WGS 84 datum and UTM 32N projection) had a cell size of 5 cm/pixel and were deemed precise enough to be used for geomorphological analysis (Figure 5).

4.6. Data Processing and Cartography

The MBES data covered 500 km^2, with track lines parallel to the coast. The multi-beam data cleaning and filtering were performed using the PDS2000 software package, while the Global Mapper software was used to construct the bathymetric map of the UTM (WGS84) Zone 32 N projection. The bathymetry was plotted on a grid at 5 m node spacing as a contour plot to display detailed bathymetric information. It was also plotted as a slope

value and an illuminated 3-D perspective view to visualise prominent features within the investigated area.

Sub-bottom profiler (SBP) data processing was performed using the Triton Elics Information suite software package. The navigation data were plotted in a geographic information system (GIS) application (DelphMap). We exported the processed seismic data in the GeoTIFF format. The side scan sonar (SSS) data processing provided the georeferenced grey-tone acoustic images of the seafloor at a resolution of 1 m.

Bathymetry was investigated by analysing the acquired multibeam data, while for the Sardinia emerged coastal sector, DTM with a 5 × 5 m cell size of the Autonomous Region of Sardinia was used.

High-resolution multibeam bathymetry was combined with the echo-types of chirp sonar data, documenting the high morphological complexity of the study area. The geomorphological map of the study area was created using ArcGIS by analysing and interpreting data at a scale of 1:5000 to obtain a highly detailed and accurate final map.

5. Results

The San Pietro Island continental shelf morphology presents a strong structural control, in accordance with the tectonic style of the passive continental margin of southwestern Sardinia. A system of normal faults, including low-angle faults, predominates and likely led to the evolution of both intraplatform and intraslope basins (Figures 2 and 4). However, on the proximal shelf, structural morphologies predominate and are often linked to volcanic processes. The distal shelf transition is abrupt and is represented by a normal fault system trending 40° N in the northern sector and N-S in the central-southern sector at depths of 80–140 m. The fault walls show the morphological evidence of a polycyclic evolution in the marine, coastal, and continental environments. The continuity of the rocky outcrops is interrupted by extensive areas with very low slopes, where the surface deposits are represented by medium-grained sands with bioclastic components and mäerl biogenic gravels. These deposits are affected by hydraulic dunes, and their granulometric features are highlighted in the backscatter side-scan sonar images. *Posidonia oceanica* is nearly absent in the western and northern coastal strips and is limited to small discontinuous areas, where seagrasses are visible on the rocks at 10–25 m depth. Starting from Punta delle Colonne and towards the east and northeast, a large *Posidonia oceanica* prairie almost completely colonizes the San Pietro Channel [57].

High rocky coasts dominate on San Pietro Island, and the highest cliffs characterize the coast exposed to the NW waves. During extreme marine events, the waves in this area reach a height of 10 m and a length of over 200 m. In the western sector (Sandalo Cape), plunging cliffs consisting compact lava rocks prevail, while pseudo-stratified pyroclastic volcanites and cliffs with abrasion platforms often masked by large subangular rockfall deposits or cones with subspheroidal boulders characterize the northern and southern coasts.

Off the fault walls, at depths of 150–170 m, a small intraplatform basin is filled with the onlapping Miocene sedimentary strata and features an isolated outcrop of volcanites. The distal platform has a very low slope located at depths of 170–200 m and composed of fine-grained sands. The sand pelitic component increases towards the open sea up to the net topographic convexity of the shelf edge located at an average depth of 220 m.

In a context dominated by volcanic and tectonic-controlled morphologies, we detected several sea-level and climate-change indicators dating back to the Upper Pleistocene and Holocene. As such, morphometric data refers to the palaeo-stages when a basal platform was located at depths of 125–135 m; morphometric and palaeontological data indicate the existence of a palaeo-lagoon at depths of 120–127 m; seismic data allows the identification of a buried palaeo-valley with a base level at a depth of 130 m; and side-scan sonar and petrographic data reveal the presence of beachrocks at depths of 45–48 m (Figure 7).

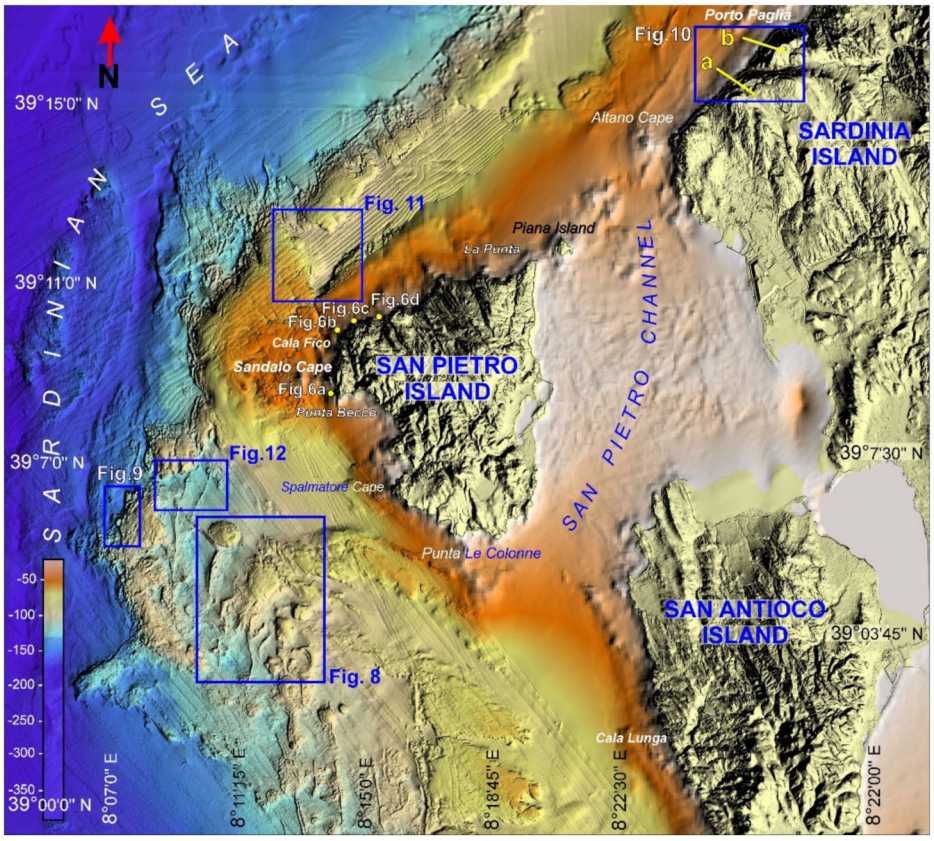

Figure 7. Location of sites depicted in the following figures.

5.1. Structural Landforms

Tectonic control on morphology is evident both in the coastline area and on the continental shelf. A fault-controlled slope affecting the Cala Vinagra comendites was recognised at the base of Punta di Cala Fico promontory, with an edge located at a depth 5 m and a base at depths of 15–25 m (Figure 6b). Two fault-controlled slopes with the same lithology were found 800 m off Sandalo Cape and Punta Becco, with an edge at 10 m depth and a base at 40 m depth. In the western sector, fault wall alignment is controlled by the tectonic lineaments trending N and 345° N, long between 1 and 3 km, revealing an organised subparallel pattern. In the northern sector, the fault walls follow a 60° N line for approximately 5 km in the same direction as the tectonic lines that control the present-day high coastline from Capo Altano to Porto Paglia (Figure 8a).

Structural surfaces, linked to the submerged ignimbrite bedrock, characterize the entire intermediate continental shelf. They are irregular and are covered by superficial sediments up to 12 km off the coast of Punta Spalmatore. The open-sea limit is represented by the edge of the palaeo-cliffs controlled by the N–S trending faults at 90 m depth. These surfaces are interrupted using their relief due to differential erosion, necks, and dikes. The structural surfaces that are slightly inclined towards SW characterise monoclinal "cuesta" reliefs found off the coast of Cala Lunga (Island of Sant'Antioco). Some sectors (e.g., off the coast of Cala Fico) present fault control. The distal platform at depths of 150–190 m presents the Miocene sedimentary sequence outcrop (Figure 3).

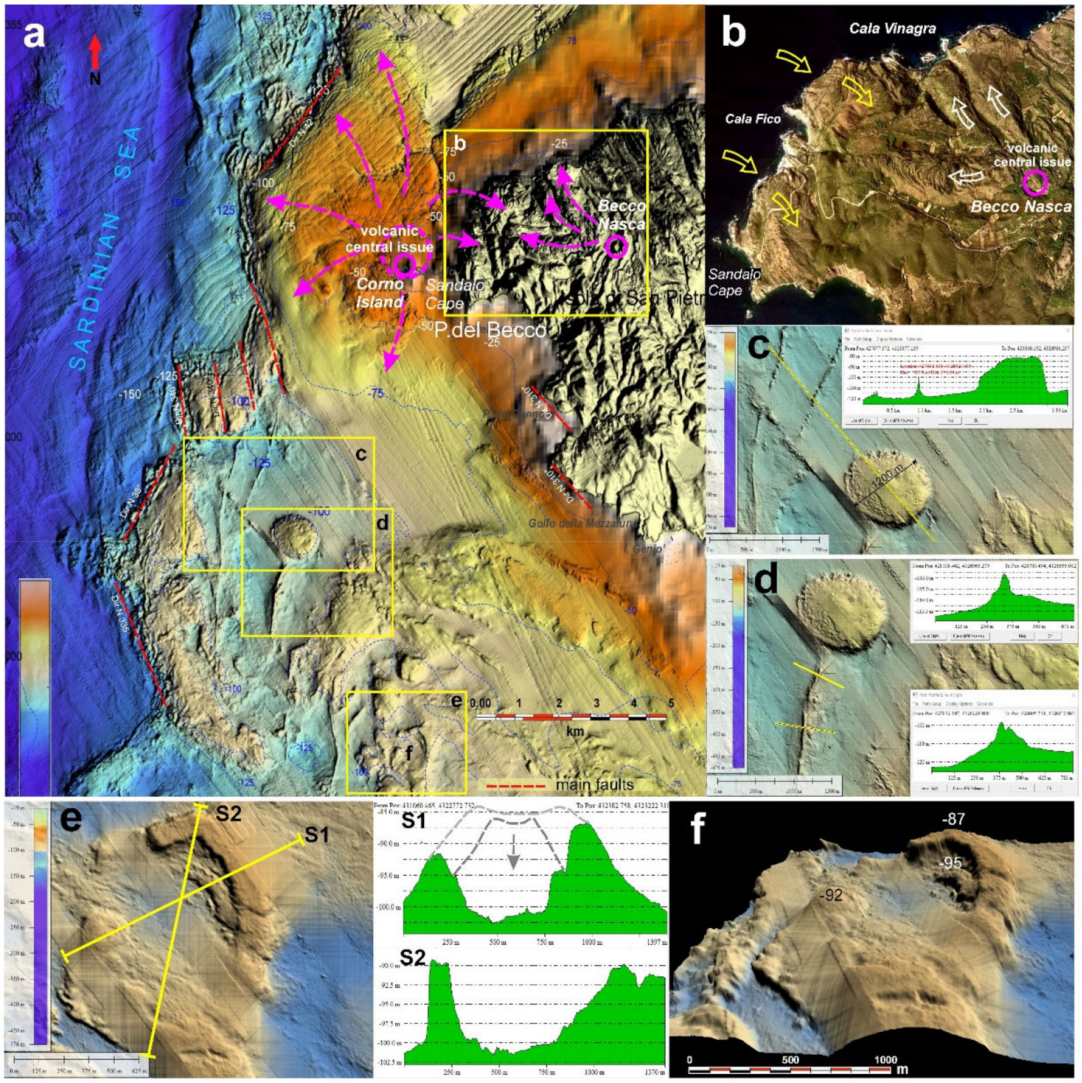

Figure 8. (**a**) Digital terrain model (DTM) from MBES data showing the drowned volcanic landforms in the continental shelf of San Pietro Island. The great volcanic edifice off Corno Island and the main fault sistems are highlighted. (**b**) Aerial photo of NW sector of San Pietro Island; the lava flow structures are evident from Becco Nasca source area (white arrows) and the lava structures from the volcanic edifice off Corno Island, currently submerged (yellow arrows). (**c**) DTM shadow relief and morphometric sections of a tabular volcanic structure (neck?). (**d**) DTM shadow relief and morphometric sections of mega-dikes, in relief due to differential erosion. These morphologies rise up to 12 m above the basal erosion surface, with longitudinal development up to 10 km. (**e**) DTM shadow relief and morphometric sections of a volcanic crater, showing a double collapse-rim structure. (**f**) Crater 3D model, the lowered internal flank and the central depression are evident.

5.1.1. Volcanic Landforms

The proximal portion of the continental shelf is dominated by the medium-Upper Miocene outcrops of acid volcanites. From a morphological point of view, numerous volcanic landforms were noted, including primary (e.g., craters or calderic depressions) and secondary landforms highlighted by differential erosion processes. The most important volcanic edifice on San Pietro Island was found on the continental shelf and occupies 37 km^2, expanding up to 6.5 km off Capo Sandalo (Figure 8a). The emission centre corresponds to the Islet of Corno, where the ignimbrite lavas (Cala Lunga Group, Middle Miocene) of Cala Vinagra were sampled. Marine erosion processes partially eroded summit members, including the Becco Nasca's comendites (Figure 8b). The residual deposit is represented by the hills of Capo Sandalo and Monte della Borrona, where the undulated morphologies

of rope lavas attest that the lavas flowed towards SE (from the sea towards the interior of the island).

A larger emission centre was found 8 km from the Gulf of Mezzaluna. It presents a sub-circular and tabular mesa morphology with a diameter of approximately 1 km (Figure 8c). The relief basis is located at a depth of 100 m, and the top is found at 82 m depth. We interpret this landform as a volcanic neck; however, it should have been a huge volcanic chimney, the largest in Sardinia. This landform might also be interpreted as a volcanic plateau, similar to those recently recognised in the western Sardinian continental shelf [58], approximately 60 km north of the study area. These landforms are typical of basic volcanites and, therefore, appear unsuitable for the volcanic context of San Pietro Island. Regardless, this hypothesis requires further investigation. We attempted sampling the rocks of the volcanic neck by dredging. However, red algae bioconstructions completely covered the rocks and prevented us from sampling. A system of eight emission centres, showing neck morphologies, is distributed along a strip extending for 5 km to the SSE of the main volcanic edifice. A crater was found about 10 km off the coast of Punta Geniò, where only the eastern half-rim is preserved. It rises from the seabed at depths of 84–100 m. This volcanic edifice indicates two phases of activity (Figure 8e), and its morphology is similar to that of the volcanic features found on the seabed in front of the Phlegraean Fields, with their unlithified light grey pumiceous cinerite [59,60] (Figure 8f). A depression with a sub-circular perimeter and a diameter of 1200 m was found 1 km to the east the crater off the coast of Punta Geniò. The depression starts at a depth of 105 m and reaches 135 m. A depression with a similar morphology was classified as a caldera [61]. The entire group of emission centres following a tangential trend is crossed by a system of mega-dikes affected by differential erosion for more than 10 m [62]. The mega-dikes have a slightly sinuous form and can extend for up to 5 km without interruption, trending from 5° N to 350° N. The only exception is represented by a dike of considerable thickness, which follows a tangential trend near the main emission centre and is oriented NW-SE. This dike was likely emplaced subsequently to the N-S-trending dike system (Figure 8d). Such extensive mega-dikes are either contemporary or were formed immediately after the rifting phase [63]. The basement rocks are often draped by thin layers of mobile sediments, which partially cover the erosional landforms engraved in the volcanic substrate.

5.1.2. Palaeo-Cliffs and Related Landforms

The morphobathymetric DTM of the studied continental shelf shows a clear discontinuity between the proximal and distal shelves. The discontinuity follows the offshore limit of the volcanites. This limit is represented by the alignments of rocky walls up to 50 m high with evident tectonic control and a prevalent orientation of 340° N.

The fault walls were subjected to polycyclic processes due to variations in the eustatic sea level in the cliff environment. Judging by the depth of the basal platforms (125–140 m), the last phase of subaerial erosion can be attributed to the LGM sea-level fall. These palaeo-cliffs are set in the volcanites, with their base locally reaching a depth of 145 m, and form plunging cliffs, similar to the modern cliffs along the Sandalo Cape coast [64].

The palaeo-cliff base is predominantly located at the shore platforms and is often affected by iso-oriented shallow erosive channels in line with the main tectonic lineaments. The basal abrasion platform has an irregular shape and is frequently covered by large sub-angular blocks of multi-decametric dimensions or by rockfall deposits. Some large blocks were found hundreds of metres from the detachment areas and recalled the evolutionary model of the block slides diagnosed in other submerged areas, such as the continental sector of the Gulf of Cagliari [34], the southern Apulian margin off the coast of Santa Maria di Leuca [65], and the Malta continental shelf [3,29,66,67] (Figure 9).The palaeo-cliff surfaces are often sub-vertical and are affected by sub-vertical fracture systems, which run parallel to the main tectonic lineaments. In some areas, sub-orthogonal joints are present and probably represent columnar cooling fracturing, similar to that in the southern coastal sector of Sardinia. The cliff summit edges are developed at depths of 80–90 m, exhibiting a

palaeo-cliff system 30–50 m high, on average. In some palaeo-cliff sectors, double ridges can be observed, pinpointing to the extensional trenches with counter-slope flanks. They were interpreted as distensional landforms and correlated with mass movement involving rotational kinematics (Figures 9b and 10).

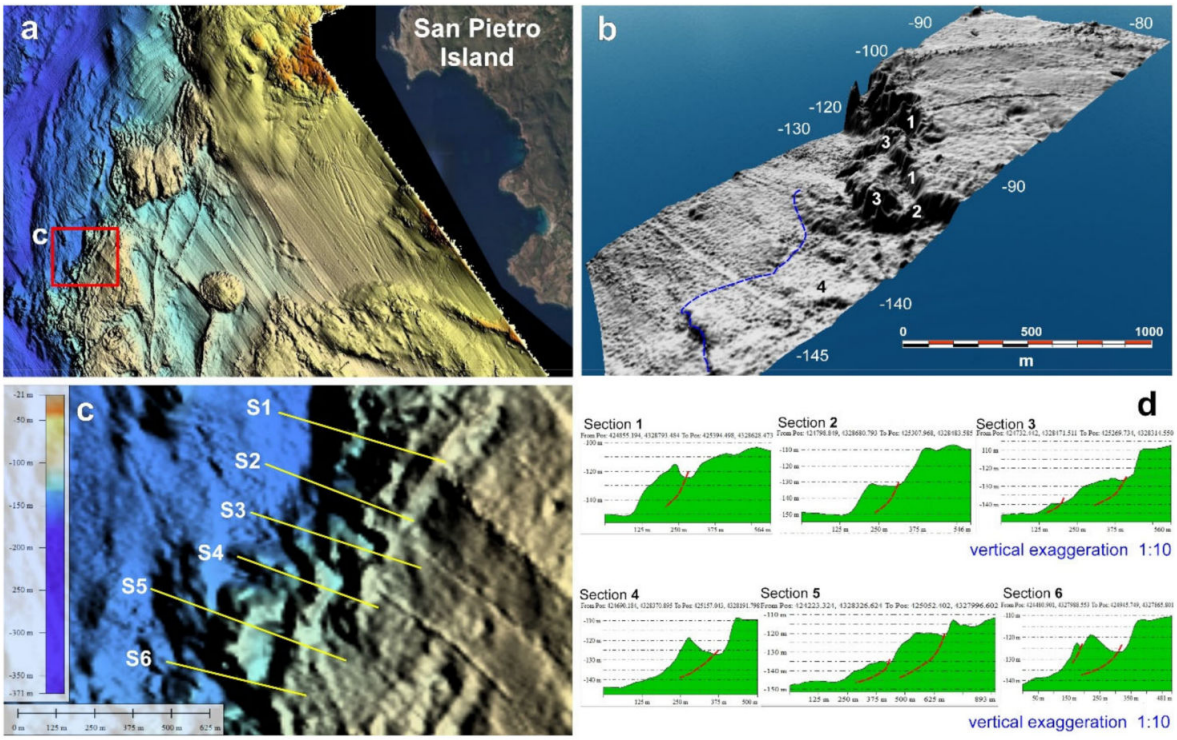

Figure 9. (**a**) DTM from MBES data showing the Last Glacial Maximum (LGM) palaeo-cliffs. (**b**) DTM 3D from MBES data showing some landslides affecting the submerged palaeo-cliffs: 1—main scarp; 2—distensional trench; 3—landslide bodies; LGM palaeo-sea-level (blue line). (**c**) detail of tectonic controlled palaeo-cliffs with localization of morphometric profiles. (**d**) Morphometric sections and hypothesized sliding surfaces (red lines).

The interpretation of the kinematics of these drowned-landslides was based on the geomorphological surveys of similar palaeo-landslides located along the coast (between Capo Altano and Porto Paglia. In this sector, large landslides with rotational kinematics were systematically observed [68]. The first landslide is located 500 m north of Altano Cape, while the second landslide has been recently found to the south of Porto Paglia (Figure 10A). Both palaeo-landslides have their foot fossilised by regression eolianites (MIS 4, MIS 3). Therefore, their movement likely occurred at a high sea-level stand during the last interglacial period (MIS 5) [9] (Figure 10D). From a morphological point of view, the first palaeo-landslide is distinguished by a complex detachment niche and is organized in two scarps. A wide trench and a counter-slope terrace are considerably lowered and are partially covered by colluvial deposits. This landslide shows the evidence of recent reactivation. The second palaeo-landslide has a detachment niche with a single scarp, a counter-slope terrace at the base of the niche, and a trench partially buried by collapsed blocks (Figure 10C,D).

In order to correlate the shapes of the submerged palaeo-cliffs with the modern (subaerial) cliffs and relate them to the landforms associated with rock falling and toppling, we carried out proximity remote sensing surveys by UAVs on some modern cliffs engraved in the same volcanic lithologies on Sant'Antioco Island and Altano Cape.

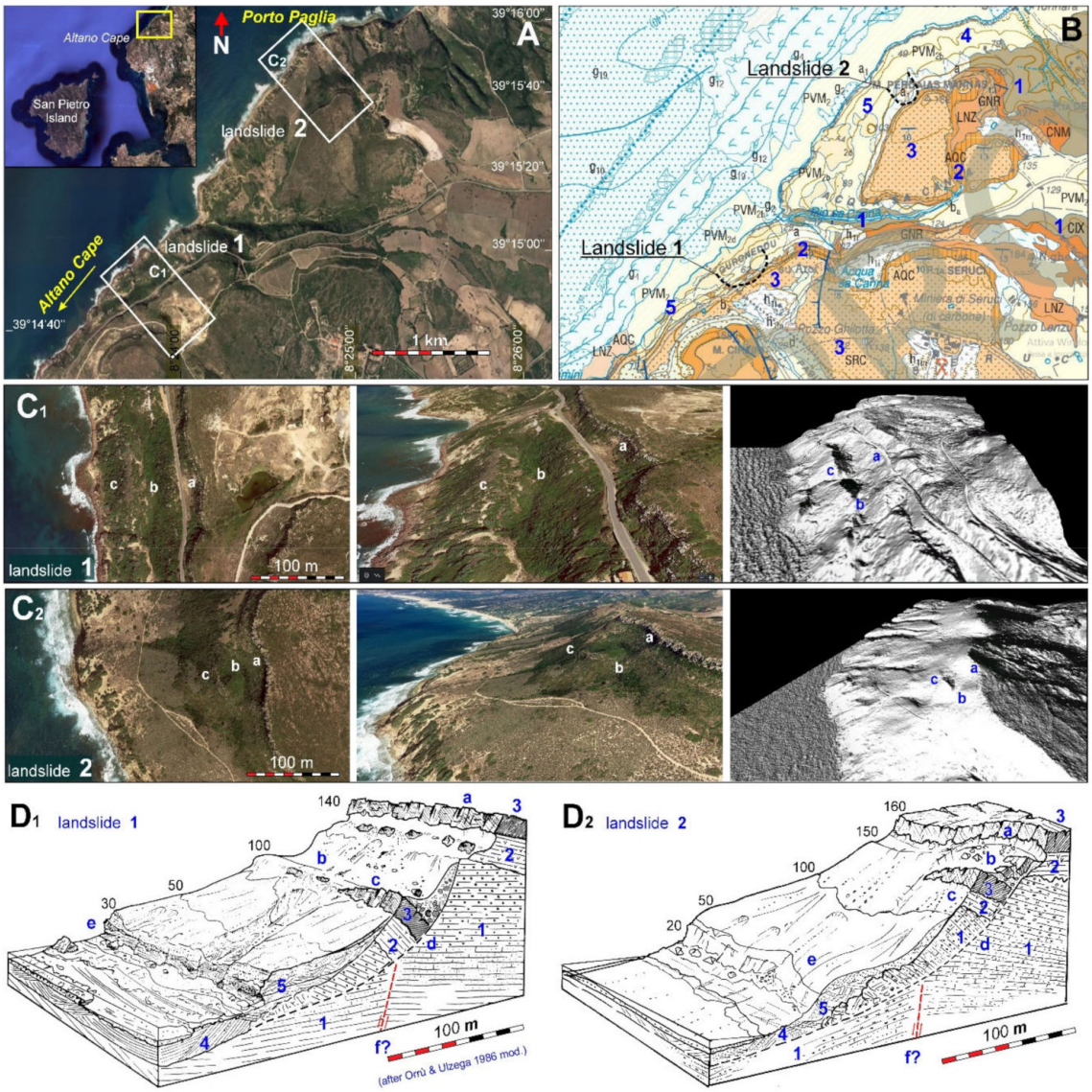

Figure 10. (**A**) Location of the studied coastal palaeo-landslides; (**B**) Excerpt of Geological Map of Italy—scale 1:50,000 Sheet 555 "Iglesias" (Pasci et al., 2015 [33]), with landslides location; (**C**) Aerial photo, photo 3D view and Lidar DTM 3D of landslide 1 ($\mathbf{C_1}$) and landslide 2 ($\mathbf{C_2}$); (**D**) Palaeo-landslide 1 3D interpretive models ($\mathbf{D_1}$) and Palaeo-landslide 2 ($\mathbf{D_2}$), showing rotational kinematics, probably due to the basal erosion during the high-stand MIS 5.5 and the subsequent foot fossilization by continental deposits of the Upper Pleistocene (MIS 4,3,2). Geolithological legend: (1) sandstones and conglomerates, Cixerri Formation—CIX (Eocene-Oligocene); (2) ignimbrites, tuffs—AQC (Middle Miocene); (3) ignimbrites, lavas—SRC (Middle Miocene); (4) eolianites (Upper Pleistocene—MIS 4-3?); (5) eolianites and colluvia—PVM (Upper Pleistocene—MIS2). Morphological legend: (a) detachment niche; (b) trench; (c) counter-slope terrace; (d) rotational sliding surface; (f) cliff engraved in the Pleistocene aeolian deposits that fossilize the landslide foot.

The ROV surveys allowed us to explore the palaeo-cliff morphology, particularly, the extensional trenches. We observed that erosional channels interrupted the continuity of the cliff, whereas the niches and hollows, formed by differential erosion, created the environments protected from the coelenterate colonies of *Corallium rubrum* (SDC—the biocoenosis of semi-dark caves). By contrast, the top surfaces of the cliffs were almost completely colonised by incrusting algae *Pseudolitophillum expansum* (coralligenous biocoenosis).

5.1.3. Fossil Palaeo-Valleys

The LGM palaeo-hydrographic network has only been partially recognised because the valley incisions are buried by very coarse-grained and gravelly bioclastic sands, especially

the mäerl facies, which inhibit the penetration of the chirp elastic signal. The only buried palaeo-riverbed that was completely identified starts from the Ria di Cala Fico and is demarcated by a fault wall that continues for approximately one km offshore trending 280° N. The palaeo-riverbed top is located at depths of 5–10 m, and the base is demarcated at depths of 20–35 m (Figure 6b). Offshore, the palaeo-drainage system is deflected by an orthogonal fault system (Figure 11).

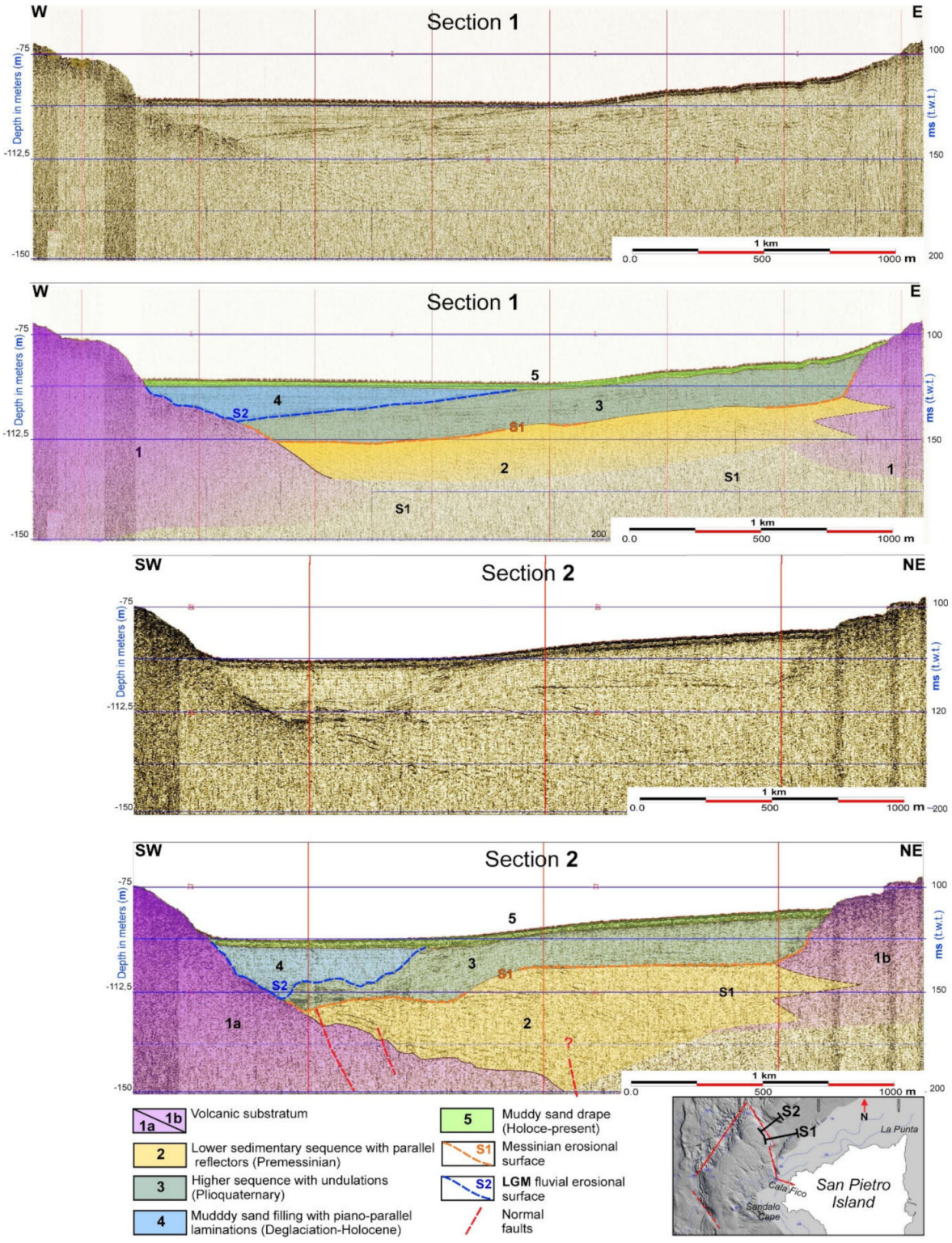

Figure 11. Seismic data of LGM palaeo-valley.

Beyond the intermediate platform with depths of 80–90 m, the morphobathymetric DTM shows a significant incision with steep rocky slopes, which is partially filled with sediments. This surface morphology possibly masks a buried palaeo-valley. To investigate this incision further, a Sparker 0.1–1 kJ seismic survey was planned and carried out. The survey proved the existence of a palaeo-valley, whose incision started in the Middle Miocene, immediately after the emplacement of the lava volcanites (Comenditi Cala Lunga Group). Subsequently, the incised valley was filled by marine sediments with inclined stratification and partially interbedded with the predominantly pyroclastic volcanites of the Middle-Upper Miocene (ignimbrites of the Cala Lunga Group) (Figure 11). The next erosive event was probably related to the Messinian low eustatic sea level [69]. In Plio-Quaternary, the palaeo-valley was completely filled by shallow-marine deposits with wavy laminations. The last identified incision down to a depth of 115 m occurred during the LGM sea-level low stand. The valley was filled by sediments originating from an environment with low wave energy, where low lighting caused a decrease in bioclastic productivity. These deep palaeo-valleys were discovered in a lower to Upper offshore environment due to the fast post-glacial to Holocene sea-level rise. In seismic images, the valley infill is represented by semi-transparent sandy mud alternating with more reflective sands of episodic storm nature (Figure 11—Section 2).

The terminal section of the palaeo-valley is enclosed within a narrow incision with walls approximately 10 m high, where we interpreted a submerged palaeo-delta at depths of 130–140 m.

5.1.4. Palaeo-Lagoon

Approximately 7 km off the coast of Punta Spalmatore, the palaeo-cliff is interrupted by a deep incision that is connected shorewards to a large depressed area at depths of 120–130 m. During the LGM sea-level low stand, this depressed area could have formed a Ria with a head bay lagoon. The palaeo-lagoon is asymmetrical, being characterised by a southern arched bank with a low slope and a deeper northern rectilinear bank (Figure 12a).

To verify the existence of this lagoon, we sampled the relevant deposits by dredging. We used a two-cylinder dredger and started from a depth of 125 m (lat 4329430.040 N, long 426914.014 E) to a depth of 129.8 m. The base was located close to the rocky wall (lat 4329755.209 N, long 426723.042 E), following a 200 m long cross-shaped church (Figure 12a,b).

The dredger sampled compact greenish-grey sandy silt, which, when washed, revealed a significant fossil content with both intact and fragmented lamellibranchs, gastropods, and serpulids (Figure 12b), marking the transition from the meso-littoral to the infra-littoral planes (Figure 12c) [30]. The sampled fauna comprised species common for lagoon and meso-littoral environments, such as the Bivalvia (e.g., *Mytilus* cfr. *Edulis, Mytilus* cfr. *Galloprovincialis, Glycymeris* sp., *Parvicardium exiguum, Pitar* cfr. *Rudis, Venus* cfr. *Casina*), Gastropoda (e.g., *Tectura virginea*, *Calliostoma laugieri*) (Figure 12d) [70], and Annelida (e.g., *Serpula vermicularis*).

Several samples were subjected to AMS (accelerator mass spectometry) ^{14}C radiocarbon analysis at the Beta Analytic laboratories (Florida, USA). The radiocarbon analysis results confirmed that the sampled rocks were deposited during MIS 2, at the beginning of the deglaciation period (Table 1) [71]. The dating of *Tectura Virginia* was the closest to that of LGM, and this species is still present in the Mediterranean Sea and some areas of the Aegean and North Adriatic Seas. The most consistent populations of *Tectura virginea* are currently present in the eastern Atlantic (e.g., Scotland, Iceland) and the North Sea (e.g., Norway, Svalbard).

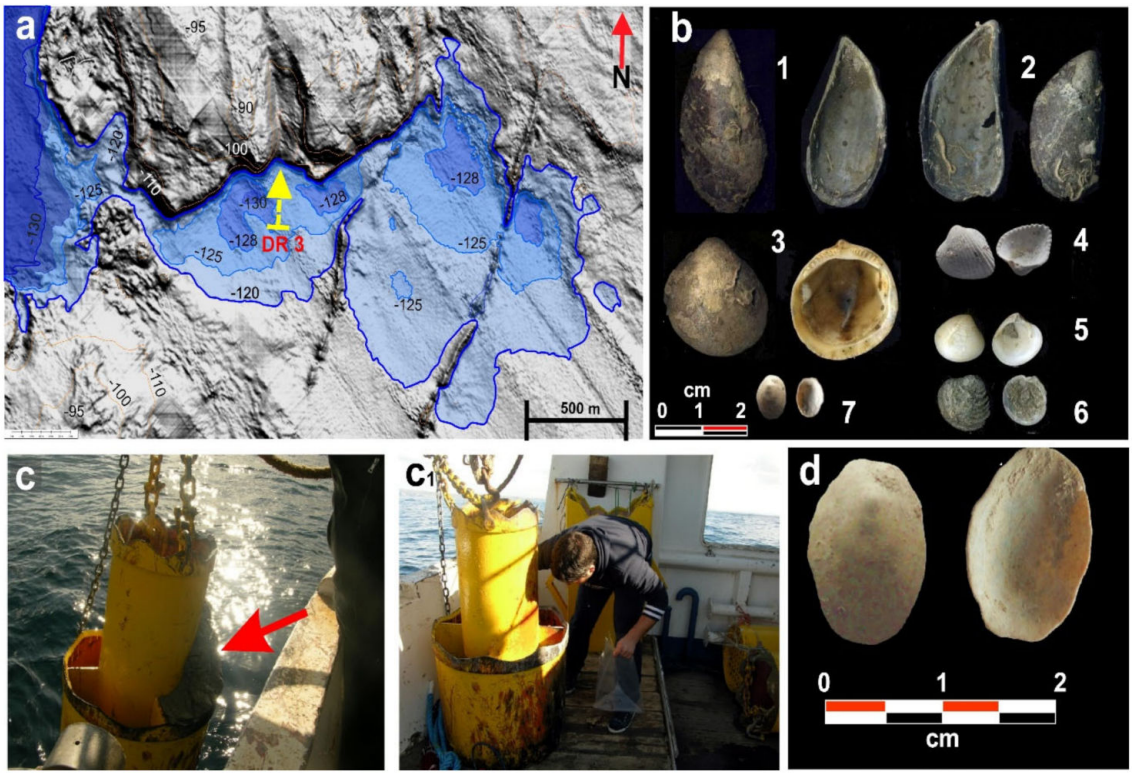

Figure 12. (**a**) Morphobatimetric DTM shadow relief showing the depression that hosted the palaeo-lagoon in the LGM; the arrow shows dredging (DR3); (**b**) sampled thanatocenosis. Bivalvia: (1) *Mytilus* cfr. *Edulis*, (2) *Mytilus* cfr. *Galloprovincialis*, (3) *Glycymeris* sp., (4) *Parvicardium exiguum*, (5) *Pitar* cfr. *Rudis*, (6) *Venus* cfr. *Casina*; Gasteropoda: (7) *Tectura virginea* (López Correa et al., 2010 [70] for the distribution of the *Tectura virginea* species). (**c**, **c**$_1$) Ascending two-cylinder experimental dredger; the arrow indicates part of the dark grey sandy silt deposit; (**d**) enlarged image of *Tectura virginea*.

Table 1. Radiocarbon dating results. The ^{14}C data were calibrated using an online version of Calib 8.1.0 (http://calib.org) and a standard marine reservoir age Bastia, Corse [71].

Lab. Code	Material	Species	^{13}C/^{12}C Ratio	Calibration Dataset	^{14}C Age (BP)	2-σ Interval of Calibrated Age (cal yr BP)
Beta-310989	shell	*Mytilus* cfr. *Galloprovincialis*	+1.7 o/oo	Calib 8.1.0	13,380 ± 60	15,014–15,688
Beta-310992	shell	*Tectura virginea*	+0.6 o/oo	Calib 8.1.0	16,350 ± 70	18,714–19,251

5.1.5. Beachrocks

Limited cemented conglomerate and sandstone outcrops were noted in the northern sector of the shelf at depths varying between 45 and 49 m (Figure 13a). These outcrops are represented by polygenic and heterometric conglomerates alternating with arenaceous microconglomerates with a feldspar-quartz matrix. The fossiliferous content is high, predominantly including lamellibranchs and gastropods, with the evidence of radiolarians and echinoids. Carbonate cementation was determined to be polyphasic, with the initial formation of magnesian calcite cement precipitated from seawater in the form of acicular crystals and followed by the cryptocrystalline globules deposited via bio-precipitation. After partial dissolution, the cementation was completed by the idiomorphic crystals of calcite deposited from freshwater. The dynamics of cementation are linked to the sea-level oscillations during an overall sea-level rise (Figure 13d). These deposits show depositional characteristics and cementation typical of a beachrock and, consequently, can be referred to as palaeo-submerged shorelines. They define the exact position of an intertidal zone. The main beachrock deposits were observed and mapped at the same depth, approximately

3 km NW of the La Punta promontory. The side-scan sonar images showed weakly inclined banks dipping seaward. Owing to the gradual basal undermining of these beachrock outcrops by strong traction currents, extensive plains are covered by unconsolidated sediments (sand) distributed in patches (Figure 13a). The top outcrop surface is denoted by a typical sub-orthogonal fracture system linked to diagenesis, favouring the occurrence of landslides at the edges (Figure 13b,c).

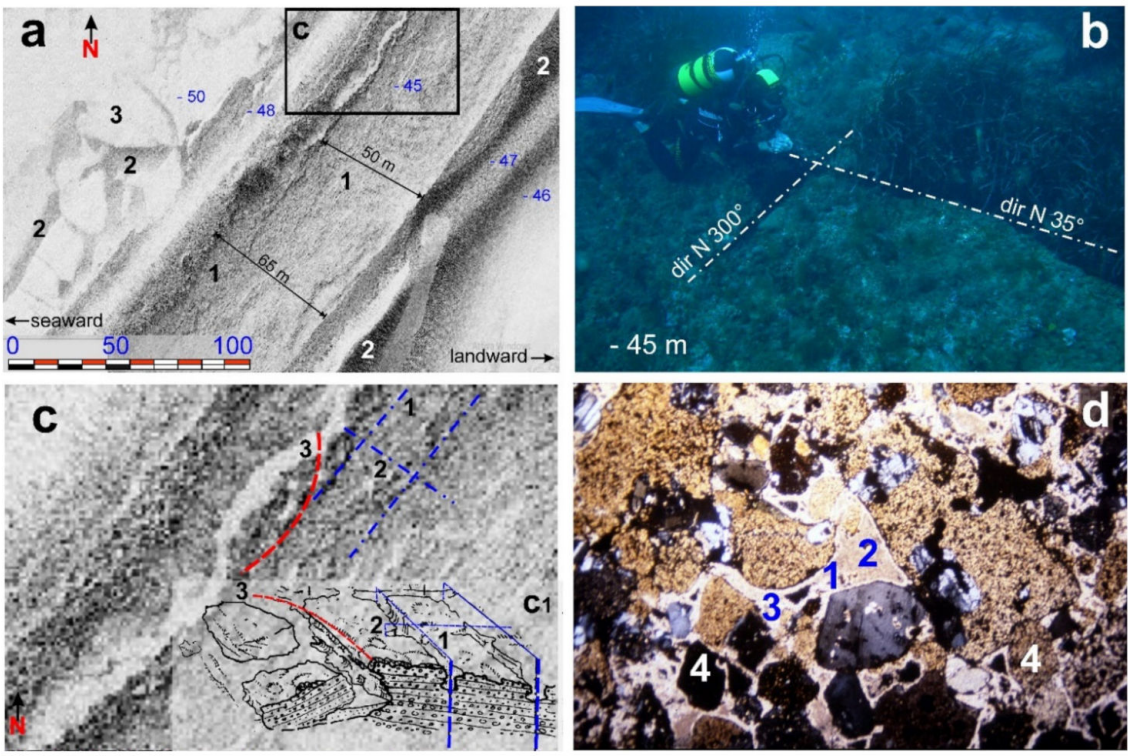

Figure 13. (**a**) The 100 kHz side scan sonar image of the beachrock a depth of 45 m: (1) Outcrop of sandstones and micro-conglomerates with carbonate cement; (2) sandpatches sedimentary structures (mäerl); (3) medium and fine grained bioclastic sands. (**b**) Seabed picture a depth of 45 m, underwater survey of beachrock fracture system. (**c**) Detail of the beachrock outcrops affected by a sub-orthogonal fracture system and by block toppling due to basal erosion: 1—35° N fracture system; 2—300° N fracture system; 3—detachment niche; (**c$_1$**) block diagram by diving survey. (**d**) Petrographic thin section of the beachrock—45 m: (1) acicular magnesian calcite coating: (2) micritic globular filling; (3) dissolution cavity with secondary clastic-micritic filling; (4) accretion of idiomorphic calcite in dissolution cavity. N.I. × 20.

6. Discussion

6.1. Last Glacial Maximum (LGM) Coastal Palaeo-Landscape

The collected data allowed us to identify the geomorphological evidence of a drowned palaeo-landscape attributable to a base level at approximately 125–145 m depth below the present-day sea level.

Continental landforms (e.g., river valleys and coastal plains), transitional environments (e.g., palaeo-lagoons and coastal landforms represented by cliffs), and associated depositional features were recognized. Different marine indicators observed at various depths helped identify a palaeo-sea-level, suggesting that the drowned palaeo-landscape formed between the LGM and early deglaciation stages [22,24]. These observations testify to the particular mobility of this continental shelf to hydro-isostatic rebounds [12], similar to those reported from the northern sector of San Pietro Island, from Fontanammare Bay to Capo Frasca (Figure 14) [54]. In our study area, the MIS 5 palaeo-sea-level indicators show relative tectonic stability [72,73], while those modelled by GIA on the southwestern Sardinian continental shelf display lower vertical displacement rates, with glacio-hydro-

isostasy constituting 0.62 mm/yr off the coast of Oristano and 0.60 mm/yr in the Gulf of Palmas [12]. Therefore, the theoretical sea-level drop attained during LGM (−120 m) could be extended by approximately 10 m (−130 m). Some research carried out on the continental shelf between Capo Pecora and Oristano indicates that the LGM palaeo-shoreline was at depths of 125–140 m [54] (Figure 14).

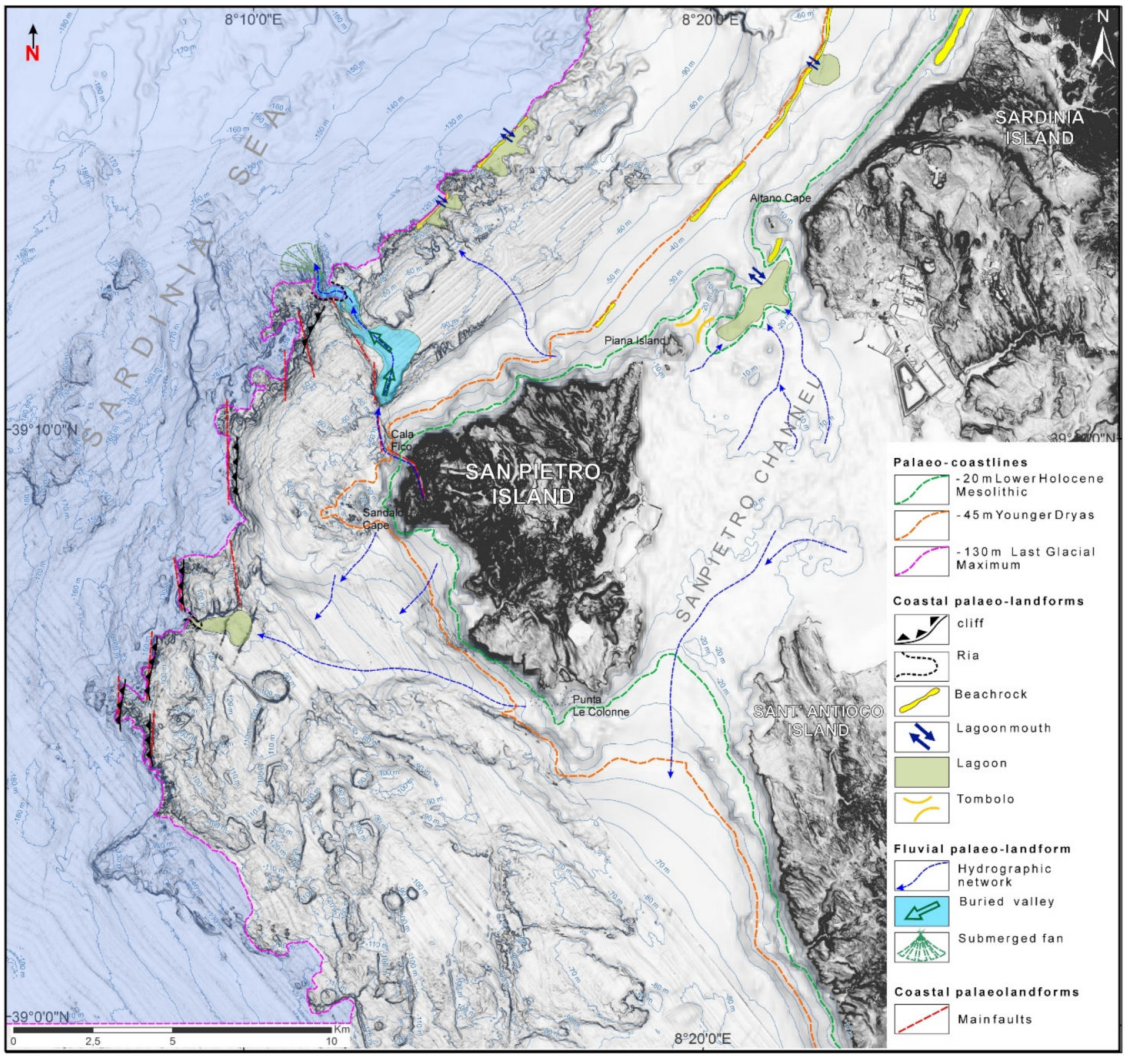

Figure 14. Geomorphological sketch of the San Pietro continental shelf. Submerged palaeo-landscape since LGM (20 ka) to 9 ka.

The LGM coastal palaeo-landscape of the study area can be subdivided into three sectors. The western sector is dominated by cliffs affected by landslides, where several large isolated blocks represent the islets and a deep Ria interrupts the cliffs' continuity and incises the head bay lagoon. The northwestern sector represents a high rocky coast with a gentle slope, probably coinciding with the lava flow fronts originating from the emission centre of Corno Island. An extensive basal wave-cut platform is situated at the base of these rocky coasts and affected by a dense system of iso-oriented erosional channels, with a prevalent direction of 330° N. The northern sector of Altano Cape is characterized by a low rocky coast with a series of beachrocks at depths of 115–120 m. It is located adjacent to two back-littoral areas with palaeo-lagoons. These beachrocks lie in a sub-parallel way and have a morphological response identical to MBES, in contrast to the beachrocks sampled at a depth of 45 m in the same sector (Figure 14).

6.2. Post-Glacial Palaeo-Landscape Evolution

Rapid sea-level rise from 130 m below the present-day sea level during the deglaciation period [22,65] likely contributed to the destabilisation of the palaeo-cliffs [74], with their geomechanical characteristics being worsened by periglacial processes. Such destabilisation could explain many massive rockfall deposits that currently cover the basal abrasion platforms.

The comparison between the geomorphological features of the subaerial coastal palaeo-landslides (Figure 10) and the identified submerged palaeo-landslides (Figure 9) has shown that both types of landslides were affected by rotational kinematics. However, the submerged palaeo-landslides have low-angle sliding surfaces, and their landslide bodies are stacked (Figure 9c), dissimilar to the present-day landslides. These differences can be linked to instability after drowning, in wave energy conditions probably very different from the present ones [75,76]. To better understand the coastal landslides kinematics in this area, it is important underline that the waves currently interacting on the coasts of western Sardinia are the most energetic in the entire Mediterranean basin. In fact, the waves measured in Alghero (northwestern Sardinia) during extreme meteorological events have a maximum height of over 10 m [77,78].

6.3. Younger Dryas Coastal Landscape

At depths of 45–48 m, we diagnosed a littoral spit in the beachrock facies. It is well preserved and extends for approximately 15 km in the northern part of the study area (from La Punta to offshore of Capo Altano). The outcrops are represented by polygenic and heterometric conglomerates with a sandy matrix and carbonate cement. The fossil content varies, and fully bioclastic levels were observed. Rock cementation indicates that a palaeo-depositional environment changed from intertidal to supratidal [52]. The outcrops are characterised by apparent erosional landforms both on the top surface and the edges (Figure 13a).

The strata are tilted slightly seaward, representing an arrangement typical of the beach sedimentary body [51]. The sedimentary structures (e.g., parallel lamination and wedge-shaped, sigmoidal, and inclined stratification) are also common in coastal environments (Figure 13b).

In Sardinia, beachrocks are found at different bathymetric levels. The deepest beachrocks are located at 95–110 m depth off La Maddalena Island, whereas the shallowest beachrocks are found at a depth of 1 m in the Gulf of Palmas and incorporate Roman pottery [30]. The latter type of outcrop constitutes thin (1–2 m) and discontinuous strata.

The beachrocks found at depths of 45–50 m are particularly thick (4–5 m) and continuous. They start in southern Sardinia, pass along eastern Sardinia, and reach the Aléria Platform in central-eastern Corsica. These littoral spits are often associated with retro-littoral areas (i.e., palaeo-lagoons and palaeo-dunes). The same beachrocks were sampled at a depth of 45 m in the Gulf of Palmas, Gulf of Cagliari, Island of Serpentara, and Gulf of Orosei. The ^{14}C analysis indicated that the beachrock ages range between 11 and 9.5 ky cal BP. In particular, the Cagliari beachrock revealed a date of 10,835 $\pm$ 170 ky cal BP [51]. As such, these palaeo-shorelines are attributed to the Younger Dryas cycle of eustatic oscillations. Off the Porto Paglia coast, the beachrock is interrupted, and the area behind it is distinguished by a sub-elliptical depression, interpreted as a palaeo-lagoon approximately 1 km in diameter (Figure 14).

6.4. Lower Holocene Coastal Palaeo-Landscape

We reconstructed the LGM coastal palaeo-landscape corresponding to the Upper Palaeolithic period. During this period, the evidence of human presence is still rare in Sardinia [79,80] (Figure 14), despite the short distance from the continent and the continuity with Corsica due to the lowered sea level during the LGM. [56]. The first evidence of human settlement in Sardinia is attributed to the Holocene [81]. The discovery of the Mesolithic site of S'Omu e S'Orku (SOMK) along the southwestern Sardinian coast, about

40 km from San Pietro Island, is of particular interest, being one of the few Mesolithic coastal sites in the western Mediterranean (Figure 15). By examining the sea-level rise curve [15,16] (Figure 16), we placed the ancient Holocene shoreline at 20 m depth. In the Holocene, the palaeo-landscape represented a vast coastal plain that extended between the present-day islands of San Pietro and Sant'Antioco and the mainland. High rocky coast was interspersed with extensive beaches with coastal dunes, as evidenced by a strip of coastal desert near Capo Altano [9]. A narrow bay was bordered by two rocky promontories between the islands of San Pietro and Capo Altano, while instead of the San Pietro canal, there existed a large bay and river mouth (Figure 14). The coastal morphological context of this part of Sardinia probably influenced the movements of the last Mesolithic groups. The human remains discovered in SOMK were dated to approximately 9 ky cal BP. The site is completely covered by red ocher and jasper artefacts (Figure 15b), the outcrops of which are found on San Pietro Island [81]. These artefacts testify to the movement of Mesolithic groups along wide beach areas close to the reliefs. Those Mesolithic groups benefited from the emerged land area between the mainland and the two small islands, where coastal lagoons favoured not only the mining of jasper and ocher but also offered food resources from sea and lagoon, especially in a period, when relatively scarce terrestrial fauna existed. The terrestrial fauna was mainly represented by the now-extinct genus *Prolagus* [82].

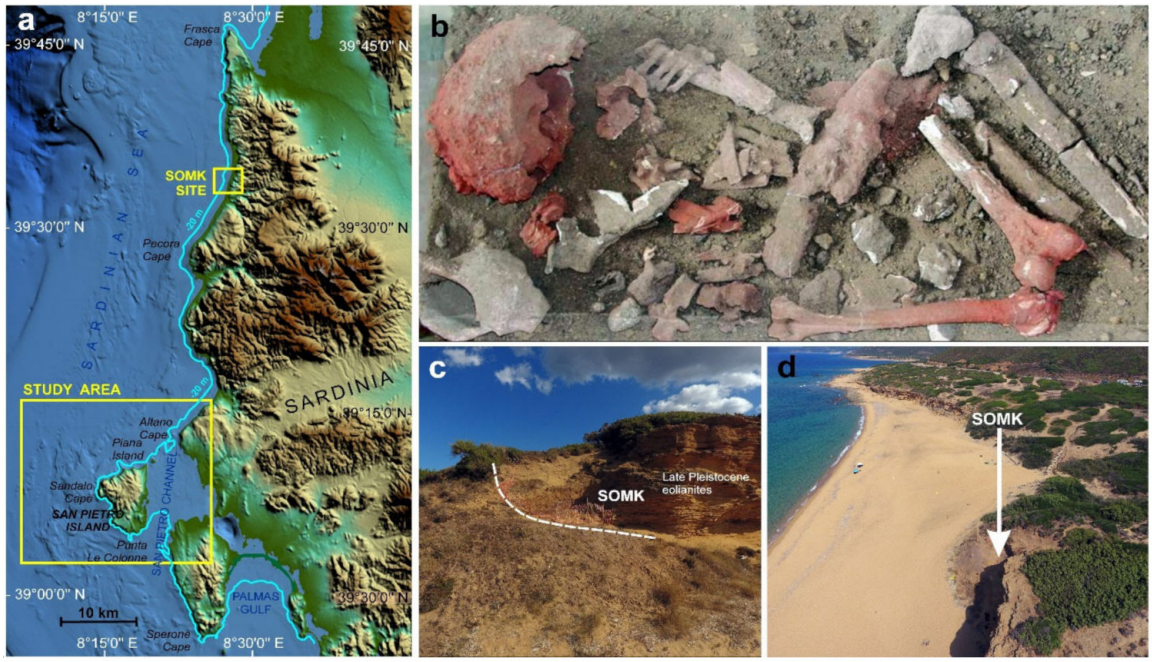

Figure 15. Mesolithic man in Sardinia west coast: (**a**) Location of S'Omu e S'Orku (SOMK) site and study area, palaeo-coastline of Mesolithic period (9 kyr BP) at 20 m. (**b**) The heavily ochre-stained skeletal remains (after Melis and Mussi, 2016 [81]). (**c**) View of SOMK Mesolithic site. (**d**) General view of the present-day position of Mesolithic SOMK site along the Sardinian west coast.

7. Conclusions

The integrated study of new geomorphological, seismic, MBS ultrasound, direct and remote-sensing UAV data allowed the evolution of the coastal palaeo-landscape of the continental shelf off San Pietro Island (southwestern Sardinia) since the LGM to be reconstructed. We found robust evidence that during LGM, the sea level was approximately 130 m depth below the present-day level, in agreement with GIA model indications (Figure 17) [12].

The morphostratigraphic investigation carried out around San Pietro Island allowed recognizing sea-floor features and landforms related to different sea-level stands during the last 22 kyr. In particular, the research highlighted the following (Figure 14):

- During the LGM the central-southern sector of the investigated area was characterized by a large promontory showing tectonically controlled high rocky coasts affected by intense fracturing and rotational landslides.
- Deep rias, set along faults, interrupt the cliffs' continuity during the same period. A large lagoon, with a peri-littoral thanatocenosis that hosted species of cold waters, formed at the bottom of one of these Ria bays (Figure 12).
- In the northern sector was there a wide river valley, while continuing towards north -east the coast became low and sandy with lagoon-barrier systems (LGM).
- The rapid eustatic sea-level rise during deglaciation, probably associated with extreme weather and sea conditions, has favoured the development of rotational landslides and debris avalanches on the cliffs (Figure 9).
- During the Younger Dryas, the eustatic oscillations between the depths of 50 and 45 m led to the construction of very thick littoral spits that extended continuously for tens of kilometers to the north (beachrocks).
- During the Holocene, the landscape comprised a vast coastal plain with lagoons that extended between the present-day islands of San Pietro and Sant'Antioco and the mainland. This landscape played an important role in the movements of Mesolithic groups along the coast. In fact, the presence of Mesolithic burials (about 40 km away), including ocher and jasper artifacts from the Island of San Pietro, shows that the Mesolithic inhabitants could reach the jasper outcrops by walking along a coast characterized by long beaches, lagoons and back-littoral dunes (Figure 15).
- Volcanic morphologies, currently not present onshore, have also been described for the first time. In particular, alignments of mega-dikes similar to those of active rift areas (Figure 8) [62].

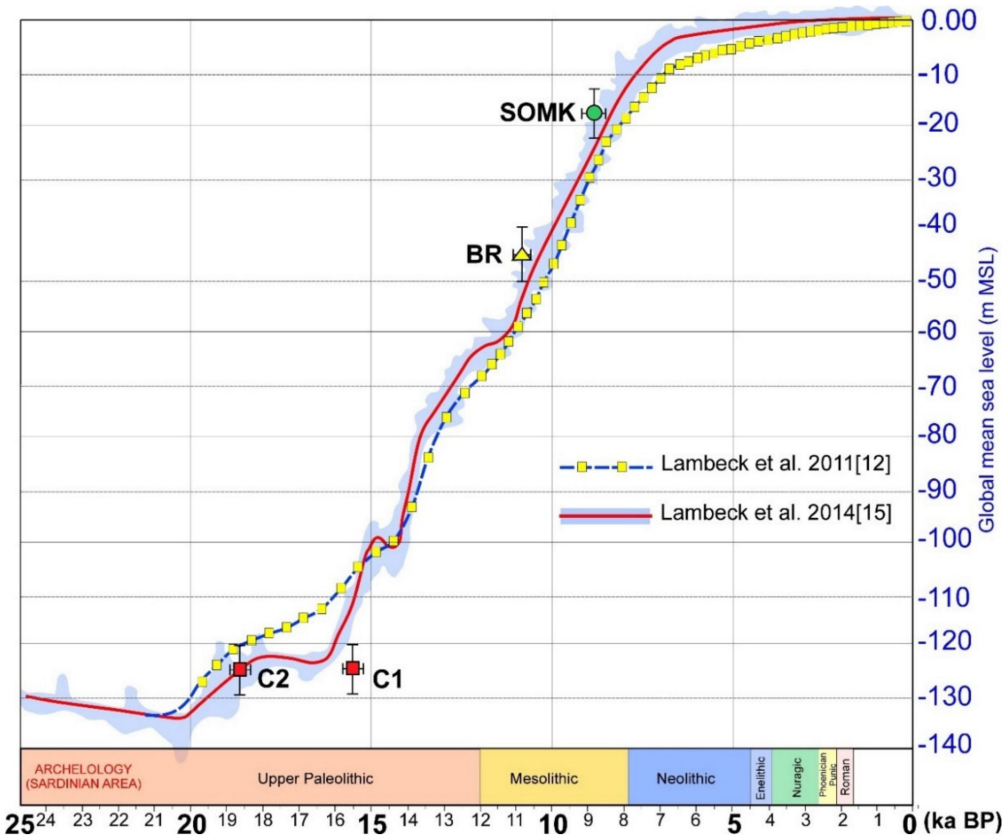

Figure 16. Relative sea-level prediction curve after Lambeck et al., 2011 [12] and Lambeck et al., 2014 [15], associated with palaeo-sea-levels indicators of San Pietro continental shelf: lagunar shells, (C1) *Acmea virginea* (gasteropoda)—18,982 ± 338; (C2) *Mytilus galloprovincialis* (Bivalvia)—15,350 ± 338 yr cal BP; BR) beachrock—10,835 ± 170 ky cal BP (De Muro and Orrù, 1998 [51]); SOMK) Mesolithic site (Melis and Mussi, 2016 [81]).

In literature, LGM palaeo-shorelines are normally investigated by focusing on single research aspects, such as seismic stratigraphy [20,21,27], lowstand depositional terraces [23] and high rocky coast evolutionary models [22]. Within our research, an effort was made to integrate a series of datasets including geological data and geomorphological evidence from both emerged and submerged areas of southwestern Sardinia. This made it possible to reconstruct the drowned palaeo-landscape in its complexity providing the means to infer evolutionary phases from the deglaciation to the present. With reference to the continental margin, the research allowed for the first time the description of geomorphological features and palaeo-landscapes associated with the LGM shoreline. Furthermore, chronological constraints for the development of peculiar landforms were achieved, thanks to the dating of correlative fossiliferous deposits.

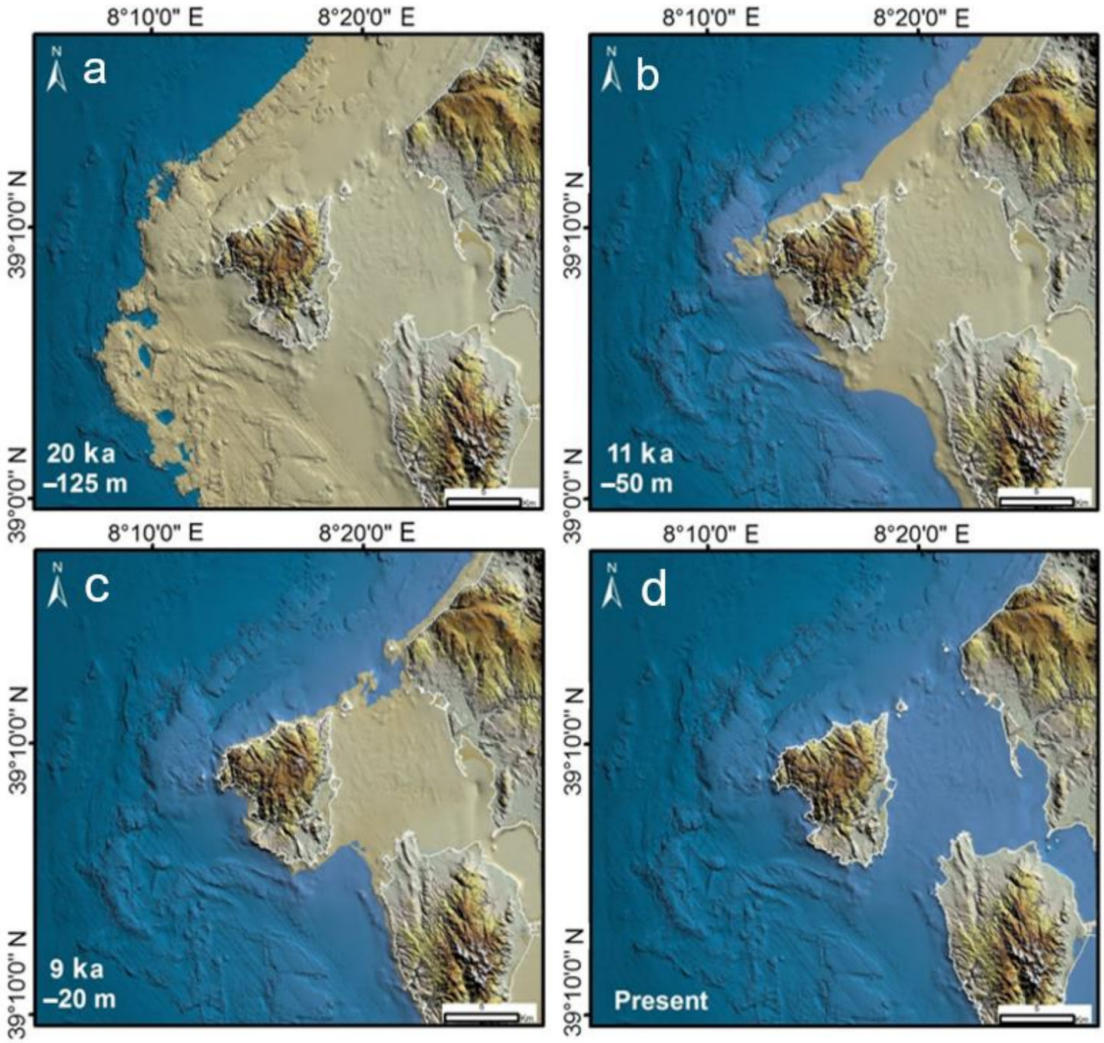

Figure 17. Reconstruction of the palaeo-landscape evolution of the San Pietro continental shelf since the LGM to present: (**a**) LGM; (**b**) Younger Dryas; (**c**) Holocene, Mesolithic; (**d**) Present.

Author Contributions: Conceptualization, G.D., L.L., M.S. and P.E.O.; methodology, G.D. and V.D.; validation, R.T.M.; formal analysis, V.D.; investigation, G.D., P.E.O. and V.D.; resources: G.D. and P.E.O.; writing—original draft preparation, G.D., L.L., R.T.M., M.S. and P.E.O.; writing—review and editing, L.L., M.S., V.D. and P.E.O.; visualization, G.D., P.E.O. and V.D.; supervision, P.E.O. and M.S.; project administration, P.E.O. and M.S.; funding acquisition, P.E.O., M.S. and R.T.M. All authors have read and agreed to the published version of the manuscript.

Funding: The study was carried out in the frame of the Project "MAGIC Marine Geohazard along Italian Coasts" funded by Italian National Civil Protection (Resp.: F.L. Chiocci—Resp. CoNISMa Unit: P.E. Orrù), of the CARG Project Geological Map of Italy, Scale 1:50,000 (Marine area)—Sheet 563 "Isola di San Pietro" and Sheet 555 "Iglesias" (Resp.: P.E. Orrù), of the SOMK Parco Geominerario 150-29.12.2017 and FdS grant number F74I19000960007 "Geogenic and anthropogenic sources of minerals and elements: fate and persistency over space and time in sediments" (Resp.: Rita Teresa Melis). The research is also part of the Project "Coastal risk assessment and mapping" funded by the EUR-OPA Major Hazards Agreement of the Council of Europe (2020–2021). Grant Number: GA/2020/06 n○ 654503 (Unimore Unit Resp.: Mauro Soldati).

Institutional Review Board Statement: Not applicable.

Informed Consent Statement: Not applicable.

Data Availability Statement: Not applicable.

Acknowledgments: We are thankful to Margherita Mussi for her precious suggestions about human heritage and georcheological implications. We are also grateful to Soprintendenza Archeologica di Cagliari for their valued support. The precious contribution of the three anonymous reviewers and of the journal editors is acknowledged.

Conflicts of Interest: The authors declare no conflict of interest.

References

1. Shackleton, N.J. The 100,000-year ice-age cycle identified and found to lag temperature, carbon dioxide and orbital eccentricity. *Science* **2000**, *289*, 1897–1902. [CrossRef] [PubMed]
2. Micallef, A.; Foglini, F.; Le Bas, T.; Angeletti, L.; Maselli, V.; Pasuto, A.; Taviani, M. The submerged palaeolandscape of the Maltese Islands: Morphology, evolution and relation to Quaternary environmental change. *Mar. Geol.* **2013**, *335*, 129–147. [CrossRef]
3. Prampolini, M.; Foglini, F.; Biolchi, S.; Devoto, S.; Angelini, S.; Soldati, M. Geomorphological mapping of terrestrial and marine areas, northern Malta and Comino (central Mediterranean Sea). *J. Maps* **2017**, *13*, 457–469. [CrossRef]
4. Prampolini, M.; Savini, A.; Foglini, F.; Soldati, M. Seven good reasons for integrating terrestrial and marine spatial datasets in changing environments. *Water* **2020**, *12*, 2221. [CrossRef]
5. Tallavaaraa, M.; Miska, L.; Korhonenc, N.; Järvinend, H.; Seppäb, H. Human population dynamics in Europe over the Last Glacial Maximum. *Proc. Natl. Acad. Sci. USA* **2015**, *112*, 8232–8237. [CrossRef]
6. Benjamin, J. Submerged prehistoric landscapes and underwater site discovery: Reevaluating the 'danish model' for international practice. *J. Island Coast. Archaeol.* **2010**, *5*, 253–270. [CrossRef]
7. Lecca, L.; Carboni, S.; Scarteddu, R.; Sechi, F.; Tilocca, G.; Pisano, S. Schema stratigrafico della piattaforma continentale occidentale e meridionale della Sardegna. *Mem. Soc. Geol. Ital.* **1986**, *36*, 31–40.
8. Orrù, P.; Ulzega, A. Carta geomorfologica della piattaforma continentale e delle coste del Sulcis—Sardegna sud occidentale. Scala 1:100,000. *STEF* **1990**, (in press).
9. Orrù, P.; Ulzega, A. Geomorfologia costiera e sottomarina della baia di Funtanamare (Sardegna sud-occidentale). *Geogr. Fis. Din. Quat.* **1986**, *9*, 59–67.
10. Miccadei, E.; Orru, P.E.; Piacentini, T.; Mascioli, F.; Puliga, G. Geomorphological map of the Tremiti Islands (Puglia, Southern Adriatic Sea, Italy), scale 1:15,000. *J. Maps* **2012**, *8*, 74–87. [CrossRef]
11. Foglini, F.; Prampolini, M.; Micallef, A.; Angeletti, L.; Vandelli, V.; Deidun, A.; Soldati, M.; Taviani, M. Late Quaternary coastal landscape morphology and evolution of the Maltese Islands (Mediterranean Sea) reconstructed from high-resolution seafloor data. In *Geology and Archaeology: Submerged Landscapes of the Continental Shelf*; Harff, J., Bailey, G., Lüth, L., Eds.; Special Publication; Geological Society: London, UK, 2016; Volume 411, pp. 77–95.
12. Lambeck, K.; Antonioli, F.; Anzidei, M.; Ferranti, L.; Leoni, G.; Scicchitano, G.; Silenzi, S. Sea level change along italian coast during Holocene and a projection for the future. *Quat. Int.* **2011**, *232*, 250–257. [CrossRef]
13. Stocchi, P.; Spada, G. Glacio and hydro-isostasy in the Mediterranean Sea: Clark's zones and role of remote ice sheets. *Ann. Geophys.* **2007**, *50*, 741–761.
14. Antonioli, F.; Ferranti, L.; Fontana, A.; Amorosi, A.; Bondesan, A.; Braitenberg, C.; Dutton, A.; Fontolan, G.; Furlani, S.; Lambeck, K.; et al. Holocene relative sea-level changes and vertical movements along the Italian and Istrian coastlines. *Quat. Int.* **2009**, *206*, 102–133. [CrossRef]
15. Lambeck, K.; Rouby, H.; Purcell, A.; Sun, Y.; Sambridge, M. Sea level and global ice volumes from the last glacial maximum to the Holocene. *Proc. Natl. Acad. Sci. USA* **2014**, *111*, 15296–15303. [CrossRef] [PubMed]
16. Rovere, A.; Stocchi, P.; Vacchi, M. Eustatic and relative sea level changes. *Curr. Clim. Chang. Rep.* **2016**, *2*, 221–231. [CrossRef]
17. Mann, T.; Bender, M.; Lorscheid, T.; Stocchi, P.; Vacchi, M.; Switzer, A.; Rovere, A. Relative sea-level data from the SEAMIS database compared to ICE-5G model predictions of glacial isostatic adjustment. *Data Brief* **2019**, *27*, 112–125. [CrossRef] [PubMed]

18. Carminati, E.; Doglioni, C. Mediterranean tectonics. In *Encyclopedia of Geology*; Elsevier: Amsterdam, The Netherlands, 2005; pp. 135–146.
19. Gattacceca, J.; Deino, A.; Rizzo, R.; Jones, D.S.; Henry, B.; Beaudoin, B.; Vadeboin, F. Miocene rotation of Sardinia: New paleomagnetic and geochronological constraints and geodynamic implications. *Earth Planet. Sci. Lett.* **2007**, *258*, 359–377. [CrossRef]
20. Maselli, V.; Trincardi, F. Large-scale single incised valley from a small catchment basin on the western Adriatic margin (central Mediterranean Sea). *Glob. Planet. Chang.* **2013**, *100*, 245–262. [CrossRef]
21. Sikora, M.; Mihanović, H.; Vilibić, I. Palaeo-coastline of the Central Eastern Adriatic Sea, and Palaeo-Channels of the Cetina and Neretva rivers during the last glacial maximum. *Acta Adriat.* **2014**, *55*, 3–18.
22. Zecchin, M.M.; Ceramicola, S.; Lodolo, E.; Casalbore, D.; Chiocci, F.L. Episodic rapid sea-level rises on the central Mediterranean shelves after the last glacial maximum: A review. *Mar. Geol.* **2015**, *369*, 212–223. [CrossRef]
23. Chiocci, F.L.; Romagnoli, C. Terrazzi deposizionali sommersi nelle Isole Eolie (Sicilia). In *Atlante dei Terrazzi Deposizionali Sommersi Lungo le Coste Italiane. Memorie Descrittive Della Carta Geologica d'Italia*; Chiocci, F.L., D'Angelo, S., Romagnoli, C., Eds.; APAT: Rome, Italy, 2004; Volume 58, pp. 81–114.
24. Caruso, A.; Cosentino, C.; Pierre, C.; Sulli, A. Sea level change during the last 41 ka in the outher shelf of southern Tyrrhenian Sea. *Quat. Int.* **2011**, *232*, 122–131. [CrossRef]
25. Casalbore, D.; Falese, F.; Martorelli, E.; Romagnoli, C.; Chiocci, F.L. Submarine depositional terraces in the Tyrrhenian Sea as a proxy for paleo-sea level reconstruction: Problems and perspective. *Quat. Int.* **2017**, *439*, 169–180. [CrossRef]
26. Lo Presti, V.; Antonioli, F.; Palombo, M.R.; Agnesi, V.; Biolchi, S.; Calcagnile, L.; Di Patti, C.; Donati, S.; Furlani, S.; Merizzi, J.; et al. Palaeogeographical evolution of the Egadi Islands (western Sicily, Italy). Implications for late Pleistocene and early Holocene sea crossings by humans and other mammals in the western Mediterranean. *Earth. Sci. Rev.* **2019**, *194*, 160–181. [CrossRef]
27. Pepe, F.; Bertotti, G.; Ferranti, L.; Sacchi, M.; Collura, A.M.; Passaro, S.; Sulli, A. Pattern and rate of post-20 ka vertical tectonic motion around the Capo Vaticano Promontory (W Calabria, Italy) based on offshore geomorphological indicators. *Quat. Int.* **2014**, *332*, 85–98. [CrossRef]
28. Furlani, S.; Antonioli, F.; Biolchi, S.; Gambin, T.; Gauci, R.; Lo Presti, V.; Anzidei, M.; Devoto, S.; Palombo, M.; Sulli, A. Holocene sea level change in Malta. *Quat. Int.* **2013**, *288*, 146–157. [CrossRef]
29. Prampolini, M.; Foglini, F.; Micallef, A.; Soldati, M.; Taviani, M. Malta's submerged landscapes and landforms. In *Landscapes and Landforms of the Maltese Islands. World Geomorphological Landscapes*; Gauci, R., Schembri, J.A., Eds.; Springer: Cham, Switzerland, 2019; pp. 117–128.
30. Orrù, P.E.; Deiana, G.; Taviani, M.; Todde, T. Palaeoenvironmental reconstruction of the Last Glacial Maximum coastline on the San Pietro continental shelf (Sardinia SW). *Rend. Online Soc. Geol. Ital.* **2012**, *21*, 1182–1184.
31. Cau, A.; Follesa, M.C.; Cannas, R.; Sacco, F.; Orrù, P.E.; Deiana, G.; Todde, S.; Cau, A.; Enrico, P. Preliminary data on habitat characterization relevance for red coral conservation and management. *Ital. J. Geosci.* **2013**, *134*, 60–68. [CrossRef]
32. Cau, A.; Follesa, M.C.; Moccia, D.; Alvito, A.; Bo, M.; Angiolillo, M.; Canese, S.; Paliaga, M.E.; Orrù, P.E.; Sacco, F.; et al. Deepwater corals biodiversity along roche du large ecosystems with different habitat complexity along the south Sardinia continental margin (CW Mediterranean Sea). *Mar. Biol.* **2015**, *162*, 1865–1878. [CrossRef]
33. Pasci, S.; Pertusati, P.C.; Salvadori, I.; Medda, F.; Murtas, A.; Rizzo, R.; Uras, V.; Orrù, P.E.; Deiana, G.; Puliga, G. *Geological Map of Italty. Scale 1:50,000. Scheet 555 "Iglesias"*; ISPRA-Servizio Geologico Nazionale: Roma, Italy, 2015.
34. Deiana, G.; Meleddu, A.; Paliaga, E.; Todde, S.; Orrù, P. Continental slope geomorphology: Landslides and pockforms of Southern Sardinian margin (italy). *Geogr. Fis. Dinam. Quat.* **2016**, *39*, 129–136.
35. Rizzo, R.; Garbarino, C.; Salvadori, I.; Patta, D.; Orrù, P.E.; Deiana, G.; Pulga, G. *Geological Map of Italty. Scale 1:50,000. Scheet 563 "Isola di San Pietro"*; ISPRA-Servizio Geologico Nazionale: Roma, Italy, 2016.
36. Lecca, L. La piattaforma continentale miocenico-quaternaria del margine occidentale sardo: Blocco diagramma sezionato. *Rend. Sem. Fac. Sci. Univ. Cagliari.* **2000**, *1*, 49–70.
37. Finetti, I.; Morelli, C. Geophysical Exploration of the Mediterranean Sea. *Boll. Geof. Teor. Appl.* **1973**, *60*, 263–342.
38. Ryan, W.B.F.; Hsü, K.J.; Cita, M.B.; Dumitrica, P.; Lort, J.; Maync, W.; Nesteroff, W.D.; Pautot, G.; Stradner, H.; Wezel Forese, C. Boundary of Sardinia Slope with Balearic Abyssal Plain—Sites 133 and 134. *Deep Sea Drill. Proj. Rep.* **1973**, *XIII*, 465–514.
39. Fanucci, F.; Fierro, G.; Ulzega, A.; Gennesseaux, M.; Rehault, J.P.; Viaris De Lesegno, L. The continental shelf of Sardinia: Structure and sedimentary characteristics. *Boll. Soc. Geol. Ital.* **1976**, *95*, 1201–1217.
40. Carta, M.; Lecca, L.; Ferrara, C. La piattaforma continentale della Sardegna. Studi geociacimentologici e di valorizzazione dei minerali contenuti. CNR, P.F. "Oceanografia e fonfi marini". *Final Tech. Rep.* **1986**, 119–218.
41. Finetti, I.R.; Del Ben, A.; Fais, S.; Forlin, E.; Klingelè, E.; Lecca, L. Crustal tectono-stratigraphic setting and geodynamics of the Corso-Sardinian Block from new CROP seismic data. *Crop Proj.* **2005**, *1*, 413–446.
42. Cherchi, A.; Montadert, L. Oligo-Miocene rift of Sardinia and the early history of the Western Mediterranean Basin. *Nature* **1982**, *298*, 736–739. [CrossRef]
43. Fais, S.; Klingele, E.E.; Lecca, L. Structural features of the south-western Sardinian shelf (Western Mediterranean) deduced from aeromagnetic and high-resolution reflection seismic data. *Eclogae Geol. Helv.* **2002**, *95*, 169–182.
44. Casula, G.; Cherchi, A.; Montadert, L.; Murru, M.; Sarria, E. The Cenozoic graben system of Sardinia (Italy): Geodynamic evolution from new seismic and field data. *Mar. Petrol. Geol.* **2001**, *18*, 863–888. [CrossRef]

45. Faccenna, C.; Speranza, F.; D'Ajello Caracciolo, F.; Mattei, M.; Oggiano, G. Extensional tectonics on Sardinia (Italy): Insights into the arc-back-arc transitional regime. *Tectonophysics* **2002**, *356*, 213–232. [CrossRef]
46. Pondrelli, S.; Salimbeni, S.; Ekström, G.; Morelli, A.; Gasperini, P.; Vannucci, G. The Italian CMT dataset from 1977 to the present. *Phys. Earth Planet. Inter.* **2006**, *159*, 286–303. [CrossRef]
47. Cioni, R.; Salaro, L.; Pioli, L. The Cenozoic volcanism of San Pietro Island (Sardinia, Italy). *Rend. Sem. Fac. Sci. Univ. Cagliari.* **2001**, *71*, 149–163.
48. Cita, M.B.; Ryan, W.B.F. Messinian erosional surfaces in the Mediterranean. *Mar. Geol.* **1978**, *27*, 193–365.
49. Haq, B.U.; Hardenbol, J.; Vail, P. Chronology of fluctuating sea levels since the Triassic (250 million years ago to present). *Science* **1987**, *235*, 1156–1167. [CrossRef] [PubMed]
50. Ceramicola, S.; Praeg, D.; Cova, A.; Accettella, D.; Zecchin, M. Seafloor distribution and last glacial to postglacial activity of mud volcanoes on the Calabrian accretionary prism, Ionian Sea. *Geo Mar. Lett.* **2014**, *34*, 111–129. [CrossRef]
51. De Muro, S.; Orrù, P. Il contributo delle beachrock nello studio della risalita del mare olocenico. Le beachrock post-glaciali della Sardegna nord orientale. *J. Quat. Sci.* **1998**, *11*, 1–21.
52. Kelletat, D. Beachrock as sea-level indicator? Remarks from a geomorphological point of view. *J. Coast. Res.* **2006**, *22*, 1555–1564. [CrossRef]
53. Carboni, S.; Lecca, L.; Ferrara, C. La discordanza Versiliana sulla piattaforma continentale occidentale della Sardegna. *Boll. Soc. Geol. Ital.* **1989**, *108*, 503–519.
54. Carboni, S.; Lecca, L. Upper Pleistocene sea-level lowstands in the continental shelf of western Sardinia (Italy). *Int. Union Quat. Res. Comm. Quat. Shorel. Subcomm. Mediterr. Black Sea Shorel.* **1992**, *14*, 57–65.
55. Lecca, L.; De Muro, S.; Pascucci, V.; Carboni, S.; Tilocca, G.; Andreucci, S.; Pusceddu, G. Note illustrative della Carta Geologica d'Italia alla scala 1:50.000, Foglio 528 Oristano. *ISPRA* **2016**, 152–156, in press.
56. Palombo, M.R.; Antonioli, F.; Lo Presti, V.; Mannino, M.A.; Melis, R.T.; Orrù, P.; Stocchi, P.; Talamo, S.; Quarta, G.; Calcagnile, L.; et al. The late Pleistocene to Holocene palaeogeographic evolution of the Porto Conte area: Clues for a better understanding of human colonization of Sardinia and faunal dynamics during the last 30 ka. *Quat. Int.* **2017**, *439*, 117–140. [CrossRef]
57. Di Gregorio, F.; Orrù, P.E.; Piras, G.; Puliga, G. Carta geomorfologica costiera e marina. Isola di San Pietro (Sardegna sud-occidentale)—Scala 1:25.000. *Boll. Assoc. Ital. Cartogr.* **2010**, *138*, 311–326.
58. Conforti, A.; Budillon, F.; Tonielli, R.; De Falco, G. A newly discovered Pliocene volcanic field on the western Sardinia continental margin (western Mediterranean). *Geo Mar. Lett.* **2016**, *36*, 1–14. [CrossRef]
59. Putignano, L.; Orrù, P.E. Note Illustrative della Carta Geologica d'Italia 1:50.000. Foglio 465—Isola di Procida. Area Marina. *ISPRA* **2010**, in press.
60. Putignano, M.L.; Orrù, P.E.; Schiattarella, M. Palaeoenvironmental reconstruction of Holocene coastline of Procida Island, Bay of Naples. *Quat. Int.* **2012**, *332*, 115–125. [CrossRef]
61. Di Vito, M.A.; Isaia, R.; Orsi, G.; Southon, J.; De Vita, S.; D'Antonio, M.; Pappalardo, L.; Piochi, M. Volcanism and deformation since 12,000 years at the Campi Flegrei caldera (Italy). *J. Volcanol. Geotherm. Res.* **1999**, *91*, 221–246. [CrossRef]
62. Keir, D.; Pagli, C.; Bastow, I.D.; Ayele, A. The magma-assisted removal of Arabia in Afar: Evidence from dike injection in the Ethiopian rift captured using InSAR and seismicity. *Tectonics* **2011**, *30*, 3–13. [CrossRef]
63. Ayele, A.; Keir, D.; Ebinger, C.; Tim, J.; Stuart, W.G.; Roger, B.W.; Jacques, E.; Ogubazghi, G.; Sholan, J. Mega-dike emplacement in the Manda-Harraro nascent oceanic rift (Afar depression). *Geophys. Res. Lett.* **2009**, *36*, 1–5. [CrossRef]
64. Sunamura, T. *The Geomorphology of Rocky Coasts*; Wiley: Chichester, UK, 1992.
65. Savini, A.; Corselli, C. High-resolution bathymetry and acoustic geophysical data from Santa Maria di Leuca Cold Water Coral province (Northern Ionian Sea—Apulian continental slope). *Deep Sea Res. Part II Top. Stud. Oceanogr.* **2010**, *57*, 326–344. [CrossRef]
66. Prampolini, M.; Gauci, C.; Micallef, A.S.; Selmi, L.; Vandelli, V.; Soldati, M. Geomorphology of the north-eastern coast of Gozo (Malta, Mediterranean Sea). *J. Maps* **2018**, *14*, 402–410. [CrossRef]
67. Soldati, M.; Barrows, T.T.; Prampolini, M.; Fifield, K.L. Cosmogenic exposure dating constraints for coastal landslide evolution on the Island of Malta (Mediterranean Sea). *J. Coast. Conserv.* **2018**, *22*, 831. [CrossRef]
68. Castedo, R.; Paredes, C.; De la Vega-Panizo, R.; Santos, A.P. *The Modelling of Coastal Cliffs and Future Trends*; Hydro-Geomorphology-Models and Trends; InTech: Houston, TX, USA, 2017.
69. Ohneiser, C.; Florindo, F.; Stocchi, P.; Roberts, A.P.; De Conto, R.M.; Pollard, D. Antarctic glacio-eustatic contributions to late Miocene Mediterranean desiccation and reflooding. *Nat. Commun.* **2015**, *6*, 1–10. [CrossRef] [PubMed]
70. López Correa, M.; Montagna, P.; Vendrell-Simón, B.; McCulloch, M.; Taviani, M. Stable isotopes (δ18O and δ13C), trace and minor element compositions of Recent scleractinians and Last Glacial bivalves at the Santa Maria di Leuca deep-water coral province, Ionian Sea. *Deep Sea Res. Part II Top. Stud. Oceanogr.* **2010**, *57*, 471–486. [CrossRef]
71. Siani, G.; Paterne, M.; Arnold, M.; Bard, E.; Métivier, B.; Tisnerat, N.; Bassinot, F. Radiocarbon Reservoir Ages in the Mediterranean Sea and Black Sea. *Radiocarbon* **2000**, *42*, 271–280. [CrossRef]
72. Ferranti, L.; Antonioli, F.; Amorosi, A.; Dai Prà, G.; Mastronuzzi, G.; Mauz, B.; Monaco, C.; Orrù, P.E.; Pappalardo, M.; Radtke, U.; et al. Markers of the last interglacial sea-level high stand along the coast of Italy: Tectonic implications. *Quat. Int.* **2006**, *145*, 30–54. [CrossRef]
73. Antonioli, A.; Lo Presti, V.; Rovere, A.; Ferranti, L.; Anzidei, M.; Furlani, S.; Mastronuzzi, G.; Orru, P.E.; Scicchitano, G.; Sannino, G.; et al. Tidal notches in Mediterranean Sea: A comprehensive analysis. *Quat. Sci. Rev.* **2015**, *119*, 1–19. [CrossRef]

74. Castedo, R.; William, M.; Lawrence, J.; Paredes, C. A new process–response coastal recession model of soft rock cliffs. *Geomorphology* **2012**, *177*, 128–143. [CrossRef]
75. Sunamura, T. A relationship between wave-induced cliff erosion and erosive force of waves. *J. Geol.* **1977**, *85*, 613–618. [CrossRef]
76. Kageyama, M.; Valdes, P.J.; Ramstein, G.; Hewitt, C.; Wyputta, U. Northern Hemisphere Storm Tracks in Present Day and Last Glacial Maximum Climate Simulations: A Comparison of the European PMIP models. *J. Clim.* **1999**, *12*, 742–760. [CrossRef]
77. Atzeni, A. Effetti idrodinamici sulle spiagge della costa occidentale della Sardegna. *Studi Costieri* **2003**, *7*, 61–80.
78. Sulis, A.; Annis, A. Morphological response of a sandy shoreline to a natural obstacle at Sa Mesa Longa Beach, Italy. *Coast. Eng.* **2014**, *84*, 10–22. [CrossRef]
79. Bini, C.; Martini, F.; Pitzalis, G.; Ulzega, A. *Sa Coa de Sa Multa e Sa Pedrosa-Pantallinu: Due "paleosuperfici" clactoniane in Sardegna*; Atti della XXX Riunione Scientifica "Paleosuperfici del Pleistocene e dell'Olocene in Italia": Firenze, Italy, 1993; pp. 179–196.
80. Mussi, M.; Melis, R.T. Santa Maria in Acquas e le problematiche del Paleo/itico superiore in Sardegna. *Origini* **2004**, *XXIV*, 67–94.
81. Melis, R.T.; Mussi, M. Mesolithic burials at S'Omu e S'Orku (SOMK) on the south-western coast of Sardinia. In *Mesolithic Burials—Rites, Symbols and Social Organisation of Early Postglacial Communities*; Grünberg, J.M., Gramsch, B., Larsson, L., Orschiedt, J., Meller, H., Eds.; International Conference Haale (Saale): Halle, Germany, 2016; pp. 733–740.
82. Melis, R.; Galheb, B.; Boldrini, R.; Palombo, M.R. The Grotta dei Fiori (Sardinia, Italy) stratigraphical successions: A key for inferring palaeoenvironment evolution and updating the biochronology of the Pleistocene mammalian fauna from Sardinia. *Quat. Int.* **2013**, *288*, 81–96. [CrossRef]